Forschungszentrum Karlsruhe
Technik und Umwelt

Wissenschaftliche Berichte

FZKA 6299

Reflood Calculations for the Projected European Pressurized Water Reactor Using SCDAP/RELAP5 mod3.1

W. Hering

Institut für Reaktorsicherheit
Projekt Nukleare Sicherheitsforschung

Forschungszentrum Karlsruhe GmbH, Karlsruhe
1999

Kurzfassung

Für den europäischen Druckwasser Reaktor (EPR), der in deutsch-französischer Kooperation entwickelt wird, wurden am Forschungszentrum Karlsruhe (FZKA) im Institut für Reaktorsicherheit (IRS) Untersuchungen zum verspäteten Fluten nach anfänglichem, vollständigen Ausfall der Wechselstromversorgung durchgeführt. Es wurde unterstellt, daß ca. 3.8 h nach Ausfall der Stromversorgung diese wieder hergestellt werden kann und somit Wasser in den Reaktordruckbehälter eingespeist werden kann. Der Einspeisezeitpunkt wurde entsprechend der maximalen Kerntemperatur zwischen 1300 K und 2300 K variiert. Ferner wurde die Verfügbarkeit der Notkühlsysteme parametrisiert. Als adäquates Simulationsprogramm wurde SCDAP/RELAP5 mod3.1.F mit den Verbesserungen der Modellierung des Wärmeübergangs beim Fluten verwendet, die im FZKA/IRS entwickelt und validiert wurden.

In allen untersuchten Fällen konnte die Kernzerstörung gestoppt werden, jedoch wurde vor dem „Quenchen“ bei anfänglichen Kerntemperaturen über 1900 K und niedrigen Flutraten Hüllrohrversagen mit nachfolgender Schmelzeverlagerung und Debris-Bildung berechnet.

Vor dem Flutbeginn wurde ein axiales Temperaturprofil im Kern von 500 -700 K/m sowie eine Aufheizgeschwindigkeit von weniger 1 K/s bei 1500K berechnet. Die Flutgeschwindigkeit im oberen Kerndrittel variiert zwischen 0.5 und 1.0 cm/s, die Dampfmassenströme werden dort, nach einem anfänglichen Spitzenwert von 5 g/(s.Stab), zu ca. 2-3 g/(s.Stab) berechnet. Die maximalen Wasserstoff Produktionsraten beim Fluten liegen zwischen 3 kg/s und 16 kg/s.

Abstract

For the European Pressurized Water Reactor (EPR), developed in a French-German co-operation, delayed flooding of the voided core has been investigated for the loss-of-offsite power scenario at Forschungszentrum Karlsruhe (FZKA) at the Institute of Reactor Safety (IRS). In this scenario it is assumed that after 3.8 h the electric power can be reestablished to feed water into the reactor pressure vessel. Parameters of the investigation are time of water injection according to the peak core temperature between 1300K and 2300K and the number of available emergency core cooling systems. As state of the art tool, the severe fuel damage code SCDAP/RELAP5 mod 3.1 Rel. F (S/R5) was used. It includes improvements with respect to heat transfer modeling in the transition boiling regime, developed and validated at FZKA/IRS.

In all cases, core degradation could be stopped, however, cladding failure with subsequent melt relocation and debris formation was calculated for initiation temperatures above 1900K and low reflood rates.

From the calculations a typical value of the axial temperature profile in the core prior to reflood is depicted as 500-700 K/m. Heat-up rates during formation of oxidation profiles are less than 1 K/s at 1500 K. Reflood velocity in the upper third of the core varies between 0.5 and 1.0 cm/s. For steam cool-down the steam flow rate has an initial spike of more than 5 g/(s.rod) and a sustained value in the cool-down phase of 2-3 g/(s.rod) of saturated steam up to global cool-down to saturation temperature. The calculated maximum hydrogen production rates rank between 3 kg/s and 16 kg/s depending on scenario and reflood initiation temperature.

Table of contents

-

List of Tables

List of Figures

List of Abreviations

ACCU	Accumulator
AIC	Absorber rods with an alloy of silver (Ag), Indium (In), and Cadmium(Cd)
AMM	Accident Management and Mitigation
BDBA	Beyond Design Basis Accident
BOC	Begin of Cycle
CB	Core Barrel
CORA	Out-of-pile severe fuel damage tests performed at FZKA, 1984-1992, http://hikwww4.fzk.de/irs/organisation/IRS1/CORA01.html
DBA	Design Basis Accident
ECC	Emercency Core Cooling
EFWS	Emergency Feedwater System
EOC	End of Cycle
EPR	European Pressurized Water Reactor, http://www.siemens.de/kwu/e/foa/n/products/s11.htm
FE	Fuel Element
FLECHT	Full Length Emergency Cooling Heat Transfer (Westinghouse), USA
FLECHT-SEASET	Full Length Emergency Cooling Heat Transfer - Separate Effects and System Effects Test (Westinghouse)
FZKA	Forschungszentrum Karslruhe, Technik und Umwelt, http://www.fzk.de/FZK2
HR	Heavy Reflector, EPR
INEEL	Idaho National Engineering and Environmental Laboratory, USA
IRS	Institut für Reaktorsicherheit, http://hikwww4.fzk.de/irs/organisation/IRS1/irs1_home.html
IRWST	In-containment Refuelling Water Storage Tank
KWU	Kraftwerk Union, Erlangen, part of Siemens, Germany, http://www.siemens.de/kwu
LHSI	Low Head Safety Injection
LOCA	Loss Of Coolant Accident
LOFT	Loss Of Fluid Test (Idaho National Engineering Laboratory, USA)
LOOP	Loss Of Off-site Power (station black-out)
LWR	Light Water Reactor
MAAP	Modular Accident Analysis Program, Fauske & Associates
MFWS	Main Feedwater System
MHSI	Medium Head Safety Injection
MSIV	Main Steam Insulation Valve
MSRV	Main Steam Relieve Valve

MSSV Main Steam Safety Valve

NEPTUN DBA Reflood test facility at PSI, http://pss100.psi.ch/~aubert/NEPTUN.html

PCT Peak core temperature

PKL Primärkreislauf, primary cooling circuit LWR-3-Loop scaled test facility at Siemens/KWU.

PSA Probabilistic Safety Assessment

PSF Projekt nukleare Sicherheitsforschung, FZK, http://psf-nt-server.fzk.de/psfhome.htm

PSI Paul Scherrer Institut, Würenlingen, Schweiz, http://pss100.psi.ch/~aubert/LTH.html

PWR Pressurized Water Reactor

PZR Pressurizer

QUENCH Resereach programme at FZK, focussed on investigations on material behavior during LWR reflood conditions: http://imf1-wt-server.fzk.de/quench/

RCP Reactor Coolant pump

RELAP5 old: Reactor Excursions and Leak Analysis Program,
presently: Reactor Leak and Analysis Program, for LWR transients and SBLOCA,
http://www.nrc.gov/RES/RELAP5/

RCSL Reactor Control, Surveillance and Limitation System

RPV Reactor Pressure Vessel

SBLOCA Small break LOCA

SCD Severe Core Damage

SCDAP Severe Core Damage Analysis Package, (USNRC code, developed at INEEL),
http://relap5.inel.gov/scdap/home.html

SCDAP/RELAP5: Coupled SCDAP and RELAP5 code to simulate reactor conditions up to SFD conditions

SFD Severe Fuel Damage

SG Steam Generator

SAMG Severe accident mutugation guidelines

SIS Safety Injection System

SR5CAP SCDAP/RELAP5 Cooperative Assessment Programm, http://www.inel.gov/sr5cap/

TMI-2 Three Mile Island Unit 2, Mitigated SFD accident,
http://www.libraries.psu.edu/crsweb/tmi/tmi.htm

USNRC United States Nuclear Regulatory Commission, http://www.nrc.gov,
USNRC-Codes (Research): http://www.nrc.gov/RES/rescodes.html

(Remark: URL-Addresses valid September 1999)

-

1 INTRODUCTION

Flooding of a reactor core is considered to be an effective way to stop an uncontrolled core damage progression if the accident has not yet led to severe fuel rod damage, i.e. for temperatures below 1700 K. For design basis accidents (DBA) the reliability of reflood has been assessed experimentally and theoretically in the last decade.

In case of beyond design bases accidents (BDBA) this strategy may also be successful. However, the experimental data base is rather scarce and additional effects at high core temperature such as oxidation, fragmentation, as well as physico-chemical interactions of the various materials in the core may complicate the simulation of reflood processes. In case of the Three Mile Island Accident (TMI-2, /1/) parts of the core experienced even temperatures above 2300K for several 1000s, time enough for clad melting, melt relocation, and debris formation. The rapid partial reflood of the degraded core initiated by reactor coolant pump (RCP) trip led to fuel rod destruction and released app. 30 % of the total hydrogen mass. So far, it cannot be excluded that the rapid reflood also led to solid material relocation. Partial core dry-out due to shut-down of the RCP contributed to formation of a molten pool in the core. The final core reflooding 500s after shut-down of RCP by means of the high pressure safety injection (HPSI) system may have influenced crust stability leading to final melt relocation into the lower plenum. Nevertheless, core degradation was stopped by flooding without loss of the reactor pressure vessel integrity.

Additional hydrogen release during reflood was also observed in in-pile (LOFT-LP-FP2, /2/) as well as in CORA out-of-pile tests /3/. Post test investigations of CORA experiments indicated that parts of the fuel rod bundle which were unaffected in tests with slow cool-down (non-flooded) became oxidized and partially degraded. Hydrogen production rates measured during reflood phases exceed significantly those measured during initial temperature escalation. A detailed explanation for this additional hydrogen release could not yet be deduced from the experimental evidence.

Presently, uncertainties mentioned above do hardly allow to extend accident mitigation measures (AMM) to beyond design basis accidents (BDBA). To investigate reflood processes in BDBA regime the experimental QUENCH programme is performed at FZKA. In a first approach single effects tests with small inductively heated fuel rod segments /4/ were performed to identify sensitive parameters. In the integral fuel rod bundle experiment (QUENCH facility /5/) up to 21 fuel rods can be heated up electrically to establish realistic boundary conditions such as initial heat-up rates, axial temperature and oxide layer profiles, as well as reflood velocities.

The large effort outlined above is necessary to assess the feasibility of AMM in BDBA in commercial reactors. In addition to the experimental activities calculations are performed to assess conditions prior to and during reflood at higher initial cladding temperatures, hence delayed reflood. For calculations state-of the art knowledge is required. Actually the only code which can

calculate reflood in the BDBA regime is the USNRC severe fuel damage code system SCDAP/RRELAP5 (S/R5, /6/) which is used at FZKA/IRS to investigate safety features during severe accident conditions /7/. Since detailed knowledge of the fragmentation process is limited a shattering model assuming a complete ablation of oxide scales is incorporated in S/R5 /6/. At FZK the thermohydraulic part has been assessed and improved against an extended experimental database (Single rod QUENCH, NEPTUN, FLECHT, PKL).

For the European Pressurized Water Reactor (EPR) the effect of delayed reflood in the BDBA regime was investigated for the Loss of off-site power (LOOP) scenario. This study is focussed on that phase of the accident sequence in which the initially well defined core geometry vanishes due to melt relocation, blockage formation, and formation of debris zones. Emphasis was put on calculation of steam and hydrogen production rates. Their release from the primary circuit are important to define appropriate hydrogen mitigation measures in the containment. Moreover, the influence of different reflood rates was investigated, assuming limited availability of emergency core cooling (ECC) systems.

Besides, reactor specific data for the QUENCH bundle experiments were derived from the calculations. Especially, initial conditions (heat-up rate, axial temperature and oxide layer profile) and reflood conditions (pressure history, flood velocities, water temperature) were extracted.

Based on the findings of the QUENCH programme, the coarse shattering model will be replaced by a more mechanistic and physically more sound one in order to improve the application range of the code with respect to development of severe accident mitigation guidelines SAMG.

2 SCDAP/RELAP5 MODELS AND OPTIONS

For reflood analyses SCDAP/RELAP5 mod 3.1 Rel.F (S/R5m31) was used. This code version has been debugged and validated against CORA, QUENCH, and Phebus tests /7/,/10/,/14/. The main improvement with respect to reflood thermohydraulics is the implementation of a better transition boiling model (s. Section 2.3, /11/).

2.1 Oxidation model

In S/R5m31 two kinds of oxidation correlation are used: early phase cladding oxidation (parabolic correlation) and late phase debris oxidation /6/. The present version does not include oxidation of the absorber rod guide tubes and water rods in fuel elements. In case of the EPR this amount can be estimated to app. 5 % of the total hydrogen mass, however, the maximum hydrogen production rate may increase more due to non-linear effects. Also oxidation of steel structures in the core region such as the heavy reflector cannot be calculated. RELAP5 heat structures used to model the lower core support plate, the upper core plate, and the upper plenum internals can neither oxidize nor melt. Due to these shortcomings the total hydrogen mass during reflood, where always sufficient steam is available (e. g. stainless steel oxidation), may be under estimated by app. 20 %.

All calculations were performed without oxidation limitation (option “Limit-off”) based on experiences gained from calculations of the Phebus FPT0 experiment /13/. The ZrO_2 failure criteria was set to 2350 K and 60 % ZrO_2 thickness, as used in validation calculations.

2.2 Shattering model

At the moment the experimental data from the single rod QUENCH experiments /5/ are not yet fully analyzed and no clear description of the basic processes is available. Two mechanisms may contribute to the observed extreme oxidation during reflood:

1. deep cracks penetrating the oxide layer as well as the adjacent metallic layer.
2. ablation (spallation) of large parts of the oxide shell or even the whole oxide shell itself.

However, one tendency can be seen: the steam quenched specimen mainly show cracks whereas the water quenched specimen show cracks as well as ablation. In a first attempt the in-built shattering model was checked. To trigger this model the following conditions have to be fulfilled:

1. Cool down rate exceeds 5 K/s for several time steps
2. Cladding temperature 1150 K < T_{Clad} < 1560 K
3. Larson-Miller: Remnant metal layer (β-Zry) < 100 µm
   (indicating thicknesses of α-Zr(O) layer app. 380µm and ZrO_2 layer app. 300 µm)

In case of oxide scales below 300 µm no shattering is calculated. In case of shattering, the whole oxide scale of the affected fuel rod segment is removed instantaneously and the new initial oxide layer thickness is set to 0.25 µm. This means that fresh metallic Zircaloy is exposed to the steam and leads to a steep increase in exothermal energy and hydrogen production.

An improved model has to consider that ZrO_2 behaves rather ductile above 1500K, and thermal stresses might not lead to large area fragmentation. At phase transition the outer oxide layers experience compressive stresses whilst in the α-Zr(O) tensile stresses occur. Radial cracks up to clad surface can occur if rapid cool-down in the transition phase takes place. However, at such rather low surface temperatures a steep temperature gradient of app. 300K across 300µm oxide layer is required to continue oxidation. Such a large value seems reasonable since the thermal diffusivity in the oxide is rather low.

2.3 Improved thermohydraulics

In previous work the capability of RELAP5 to calculate reflood conditions has been assessed with respect to different models. The transition boiling model ($75K < \Delta T_{wall\ superheat} < 600K$) has been corrected and its prediction with respect to low mass flow rates significantly improved /11/. Based on validation calculations the most significant effect was found to be an enhanced steam production due to higher heat transfer and a better prediction of the quench time.

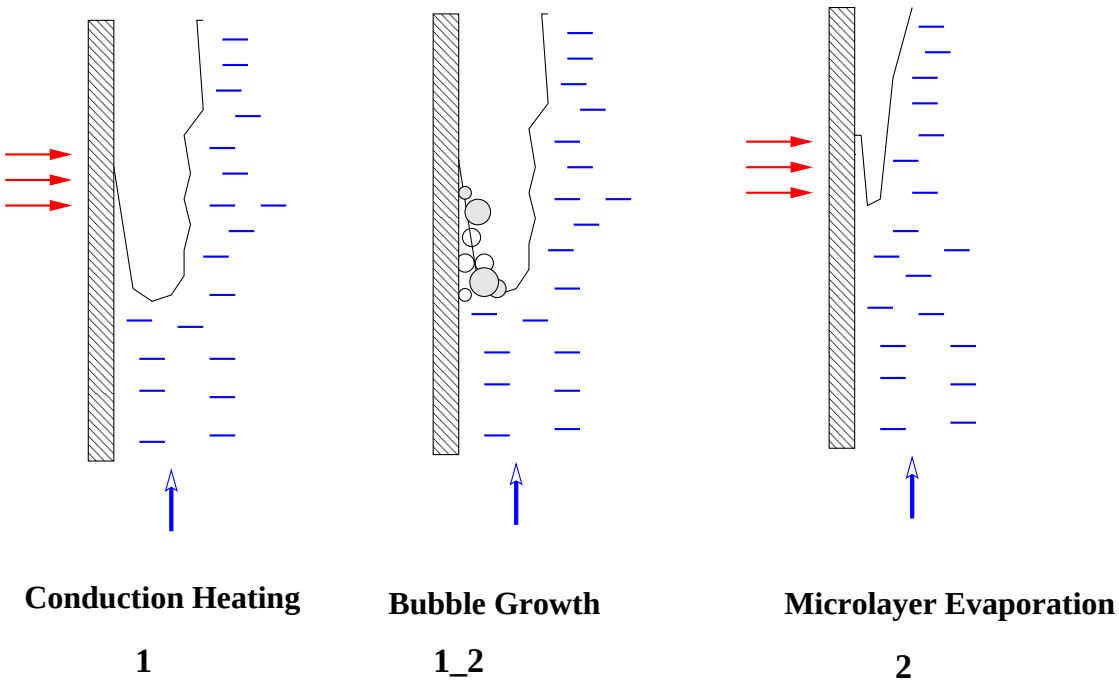

Figure 2.1 Schematic description of suggested phases in the transition boiling model /12/.

Based on the semi empirical transition boiling model proposed by Chen /12/, three phases (s. Figure 2.1) named conductive heating, bubble growth, and micro-layer evaporation (leading to

local dry out) occur sequentially. First and last phase are linked by bubble formation where the heat to form the bubbles is assumed to come from the superheated liquid layer so that the heat flux at the wall surface vanishes. Such mechanisms may also occur in the film boiling regime ($\Delta T_{wall\ superheat} > 600K$) where also dispersed droplets may cause local and temporal quenching of the oxidized cladding surface. In this regime, the heat transfer values are still over estimated and work is under way in Korea, Switzerland, and FZKA to improve the code.

Nevertheless a microscopic picture is difficult to realize for a plant size model, where minimum zone sizes are about 0.3 m and several thousands of rods are modeled by one representative rod. Under these assumptions the shattering model should give an upper bound for the new metallic surface area exposed to the steam atmosphere.

Presently, S/R5 does not include a direct link between the description of fuel rod behavior (shattering model, s. section 2.2) and the conditions in the fluid channel, except for surface temperature level ($1150K < T < 1500K$) and cool-down rate ($> 5K/s$). In reality, solid state behavior and thermalhydraulics are coupled closely together depending on the interface conditions.

A more sophisticated model has to consider the experiences gained in modeling the thermal hydraulic conditions during reflood /11/ as well as mechanical and physico-chemical experimental findings from the QUENCH programme.

3 CONDITIONS FOR REFLOOD ANALYSES

Accident analyses were performed using SCDAP/RELAP5 mod3.1 (s. Section 2) for several scenarios leading to severe fuel damage conditions /7/. In agreement with Siemens/KWU /9/ a reflood scenario was selected based on the Loss-of-offsite power (LOOP) scenario (s. Table 3.1). It assumes a total loss of alternating current (AC) and the diesel engines. Therefore, no injection system is available to flood the core except for the passive accumulators. In /7/ a series of results of calculations for Loss of Coolant Accidents (LOCA) including the surge line rupture and a Loss-of-offsite power (LOOP) scenario are given. The LOOP reflood scenario differs only by activation of the ECC systems at selected core conditions.

Table 3.1 Brief summary of all starting conditions for the different scenarios which were analyzed with S/R5 mod 3.1 to allow for comparison with other code calculations.

Initial events	Name	Leak size (cm^2)	Leak-Position	2^{nd} side cooldown	2^{nd} side manual cooldown	EFWS	1^{st} side depress	ECC-activation
LOCA	0.5F	2380	cold leg 2	No	No	No	No	No
	0.1F	477	"	No	No	No	No	No
	x18	180	"	5.5 MPa	No	Yes	No	No
SBLOCA	x5	5	"	5.5 MPa	No	Yes	3 valves	No
	x50	*50*	*"*	*6.0 MPa*	*Yes / No*	*Yes*	*No*	No
Surge line rupture	*SL (2F)*	*951*	*hot leg 1*	*6.0 MPa*	*No*	*Yes*	*3 valves*	No
Loss of off-site power	LOOP	----	----	5.5 MPa	Yes / No	No	3 valves	No
Loss of off-site power	**LOOP Refl**	**----**	**----**	**5.5 MPa**	**Yes / No**	**No**	**3 valves**	**1 – 4 LHSI 1 – 4 MHSI**

3.1 Plant representation

The S/R5 input deck for an adequate plant representation /7/ is based on a RELAP5 input deck from Siemens/KWU. It includes all significant primary circuit components using a two loop approach. Secondary side components include systems to simulate LOCA and LOOP accidents starting from normal operation. The necessary parts of the reactor control, surveillance and limitation system (RCSL) are realized by RELAP5 trip logic and control variables. All piping is coupled with 1-d heat structures to achieve realistic boundary conditions. This EPR input deck has been improved by modeling the emergency core cooling systems (ECC, Section 3.1.2) as well as its activation by simulated operator interaction.

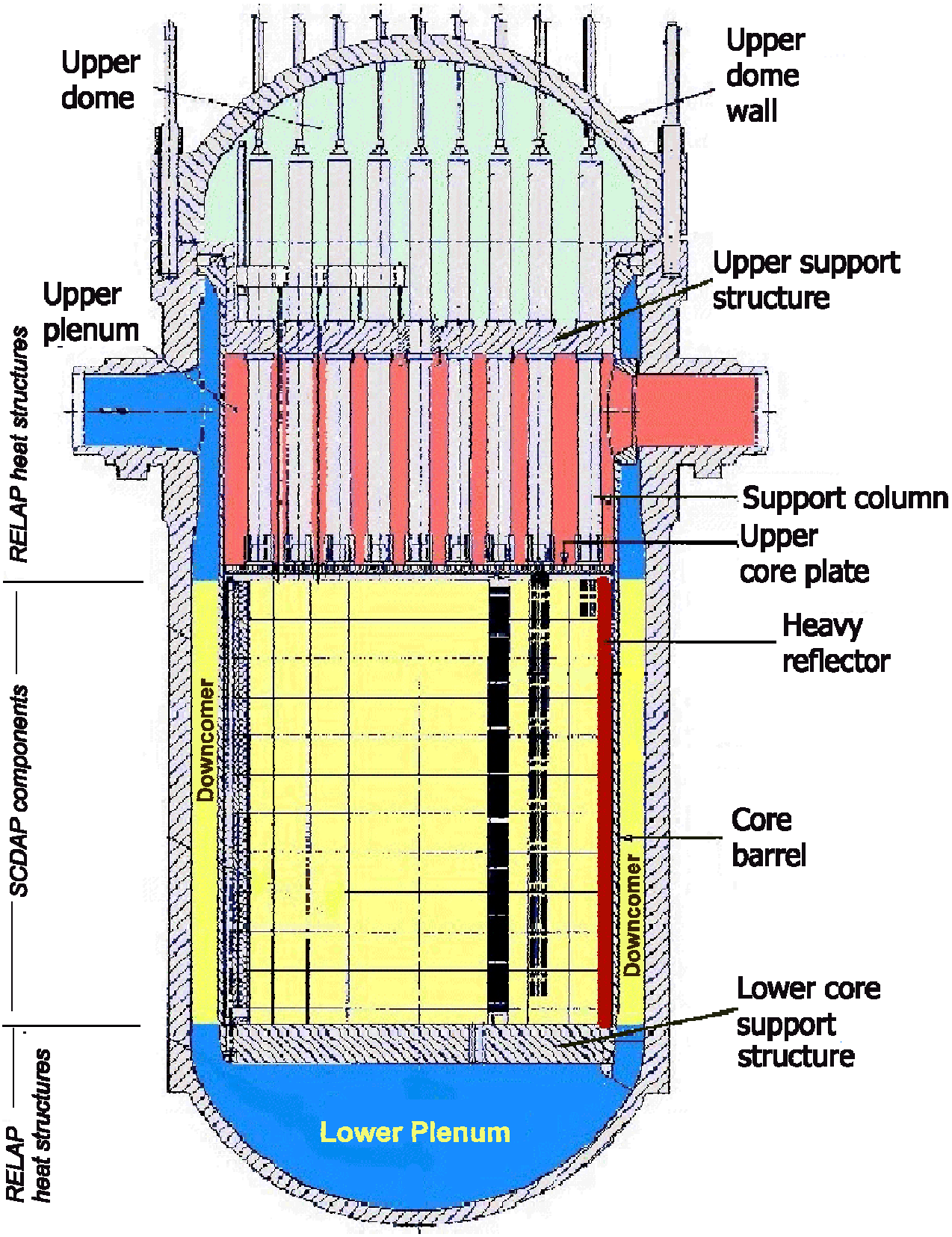

Figure 3.1 Schematics of the EPR reactor pressure vessel including all modeled internals as well as their representation by SCDAP components (core, HR, cylindrical part of RPV wall) and/or RELAP5 heat structures.

3.1.1 Core modeling

The reactor core (s. Figure 3.1) is divided axially into 16 zones, 14 zones representing the active core, each 0.3 m long. In radial direction five rings (s. Figure 3.2) plus a bypass channel in the heavy reflector allow detailed analyses even in the late phase of severe core damage accidents (s. Figure 3.3). The cross flow junction located between adjacent rings at each elevation have to be assumed closed prior to reflood initiation to avoid numerical pressure oscillations due to the solution algorithm of the momentum equation. However, this simplification does not affect results of the calculations strongly because temperature and fluid flow variations are much larger in axial than in radial direction. Only in case of very rapid oxidation and low mass fluxes the inhibited steam exchange may affect heat-up rates in the upper part of the core.

In each core channel one representative fuel rod plus one absorber rod is simulated. Radiative heat exchange is modeled between adjacent rings based on the interface areas of the FE geometry. The fifth ring is surrounded by a SCDAP shroud component simulating the heavy reflector (HR) as well as the core barrel (CB). The outer surface of this shroud component is in contact with the downcomer (DC) which is surrounded by another SCDAP shroud component simulating the reactor pressure vessel (RPV) wall, allowing radiative heat transfer across the downcomer. This is important for radial heat flux calculation in the late phase modeling to investigate the melt down behavior of HR and CB.

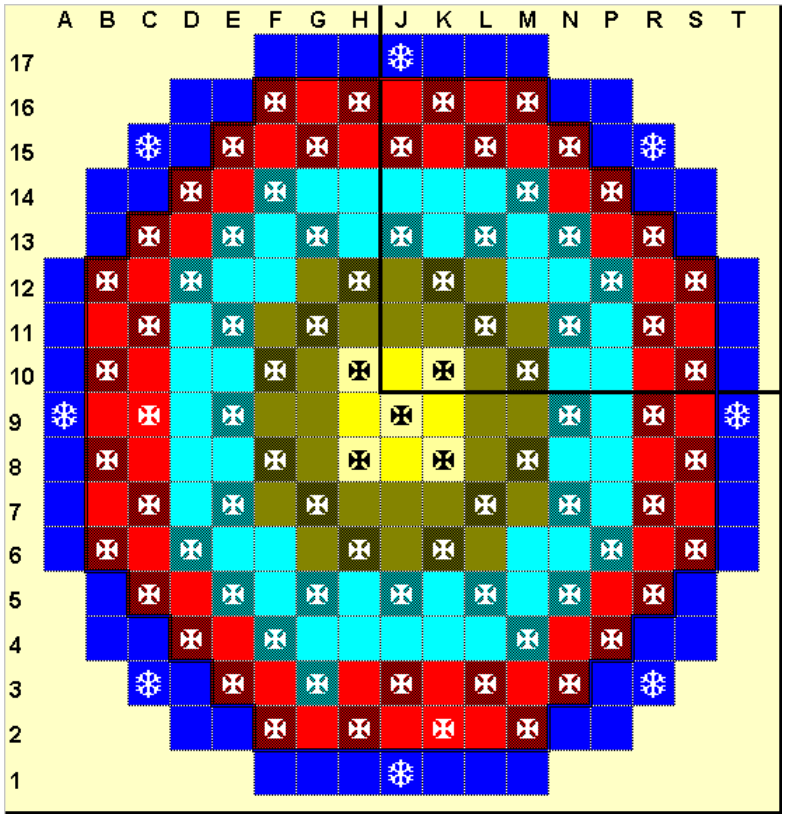

The RPV internals above (upper core plate) and below (lower core support structure) the core are modeled as RELAP heat structures (s. Figure 3.1) to ensure consistent 5 channel discretization in radial direction.

Figure 3.2 Radial core discretization for reflood analyses

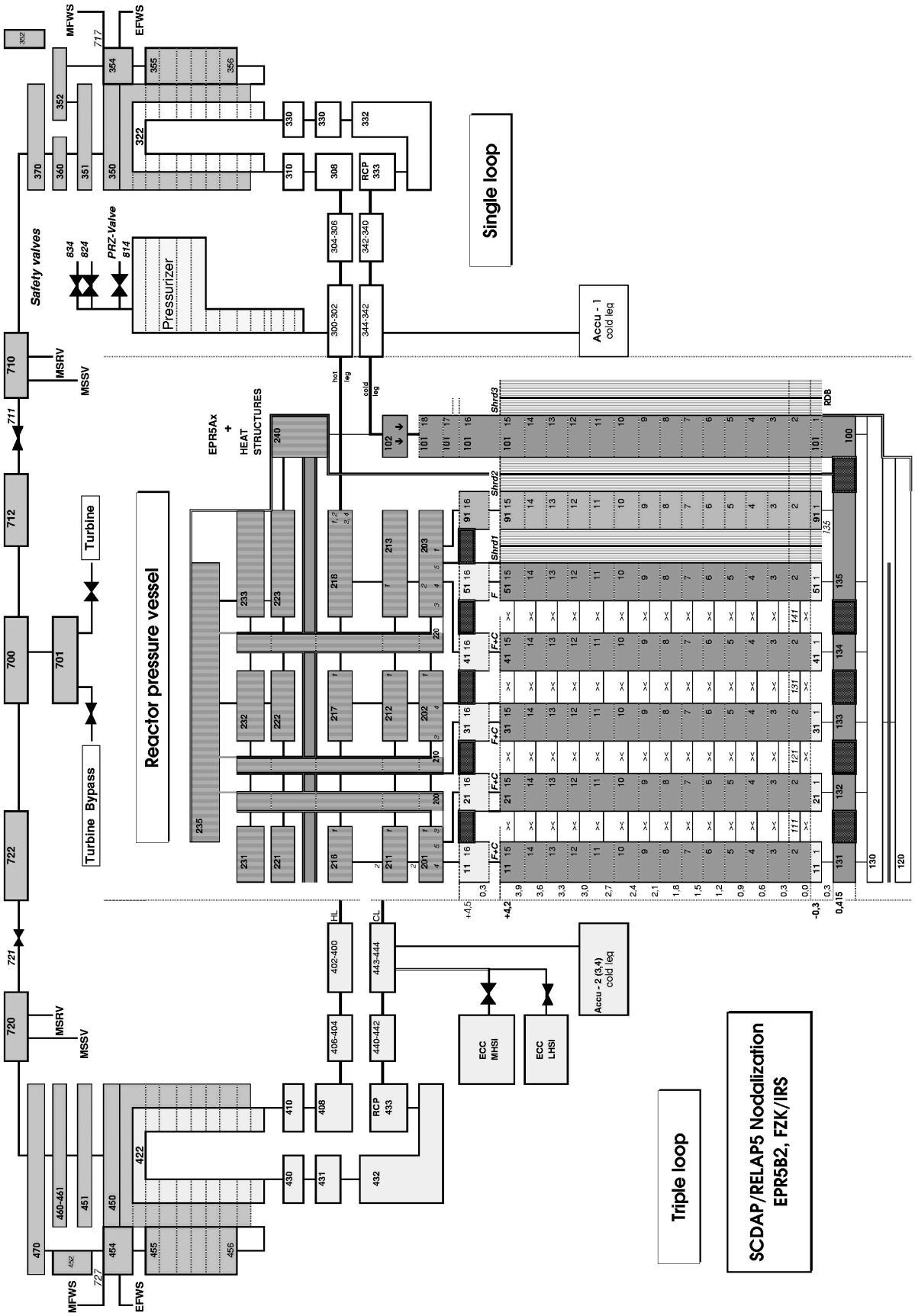

Figure 3.3 Plant nodalisation scheme used for reflood calculations with S/R5m3.1F including accumulators as well as emergency core cooling (ECC) systems.

The local power in the core is derived from decay heat (s. Figure 9.1) and is distributed according to a given axial (s. Figure 3.4) and radial power profile (s. Table 3.2) . In this study a begin of cycle (BOC) situation is simulated. Since the radial power profile only changes less than 10 % in the BOC state, as can be seen in the 6th column ($P_{(rad)}$ rel BOC) of Table 3.2, it can be assumed as flat in radial direction. In the last column the individual radial fuel rod power factor used in the calculations is outlined. This radial profile was selected for investigations focused on the melting of the HR.

Table 3.2 Core configuration and radial power profile for the BOC state of the core

Ring	Fuel elements	Number of fuel rods	FE with AIC	Number of AIC rods	$P_{(rad)}$ rel BOC	$P_{(rad)}$ scaled fuel rod
1	9	2376	5	120	1.04	0.0370
2	36	9504	12	288	1.04	0.1480
3	64	16896	24	576	1.09	0.2684
4	76	20064	40	960	1.01	0.3281
5	56	14784	8	192	0.81	0.2185
Sum	***241***	***63624***	***89***	***2136***		***1.0***

The axial power profile for this study is given in Figure 3.4. The slope deviates slightly from the chopped cosine shape normally used in severe fuel damage studies but this does not affect conditions during reflood. The difference between begin of cycle (BOC) and end of cycle (EOC) in Figure 3.4 shows the effect of burn-up during the cycle and may also influence the boil-down rate as well as steam production during reflood in the lower part of the core. Since the power variation is about 20 % reflood calculations will be repeated in a next step for EOC conditions with S/R5 mod3.2 (S/R5m32) in close cooperation with Siemens/KWU.

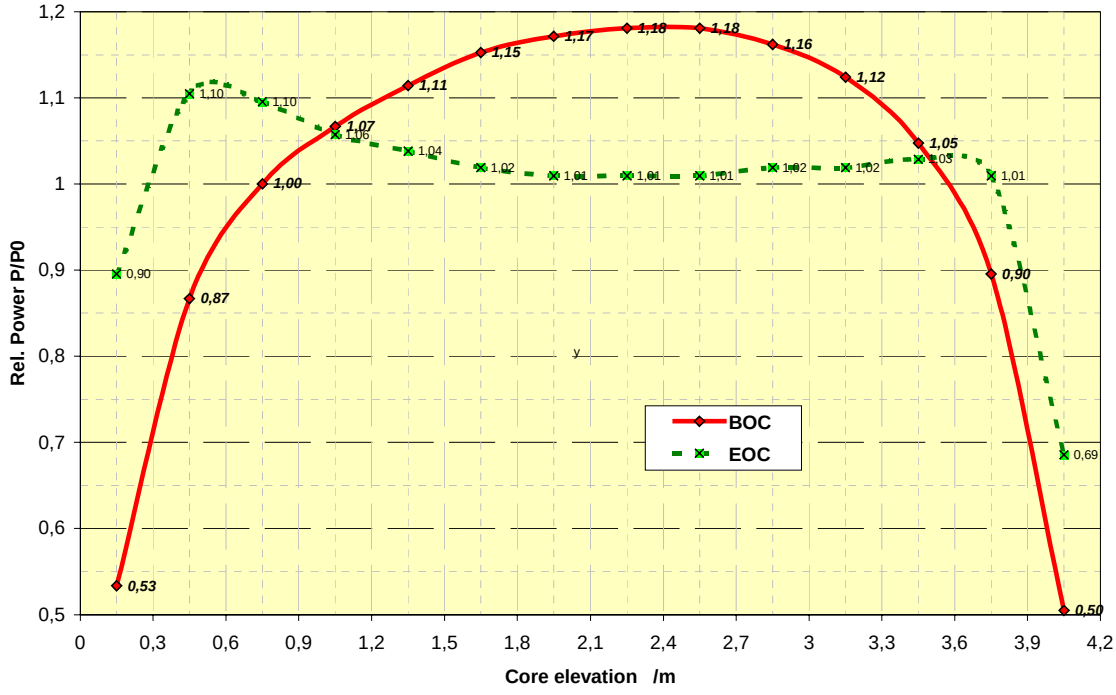

Figure 3.4 Axial power profile for two core states BOC and EOC. The BOC profile has been used in this study.

3.1.2 Primary system

The primary system is realized as a 2 loop-model, one representative loop (single loop, Loop 1,) containing the pressurizer and a three-fold loop (triple loop, Loop 2). Four accumulators are modeled to avoid scaling problems in the accumulator surge line. For the reflood study accumulators are calculated to be already emptied.

All pipes, the valves, as well as the pressurizer are connected to heat structures to get information about heat-up during depressurization and boil-down. At outer side of the RPV adiabatic boundary conditions are assumed. The pressurizer simulation is based on a nodalisation used for LOCA and DBA transient analyses at Siemens/KWU.

The volume control system is simulated as pressure control valve (814) to a time-dependent volume, which is closed at time of loss of AC-power. The three pressurizer safety valves which open at different system pressures have been adapted to one pressure control valve (824), which becomes active during overpressure states before scram and one depressurization valve (834), which simulates the other two safety valves (s. valves 824, 834 in Figure 3.3)

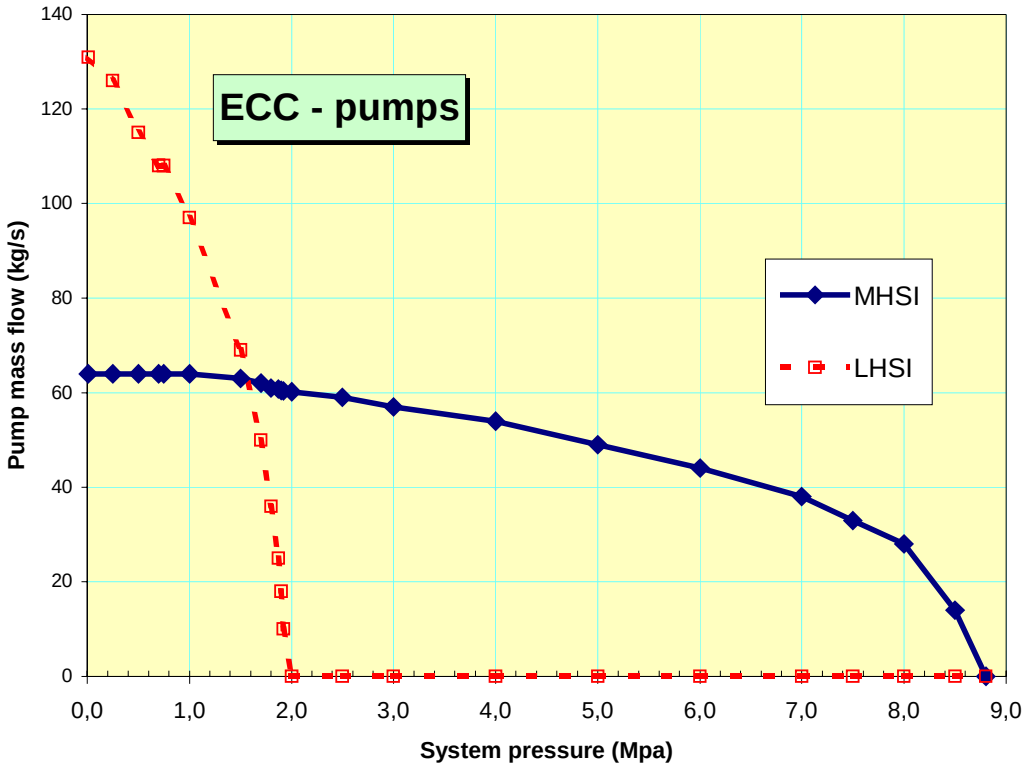

Figure 3.5 Pump curves for one medium head safety injection (MHSI) and one low head safety injection (LHSI) system.

The adequate simulation of the emergency core cooling pumps is based on ECC pump curves supplied by Siemens/KWU (s. Figure 3.5). Since only the behavior of core internals is of interest

complete groups of medium head safety injection (MHSI) system and low head safety injection (LHSI) system were modeled at the triple loop. The most important item is to model the injection rate as function of system pressure and pump head. The pumps are connected directly to the primary system cold leg.

In the LOOP scenario steam is injected for condensation into the in-containment refueling water storage tank (IRWST) which could not been modeled in RELAP5 due to numerical problems caused by condensation. Therefore, the containment pressure was set constantly to 0.2 MPa. To activate the ECC system a maximum value for the peak core temperature (PCT) was set. It is not very important in which axial or radial zone the criteria is reached firstly. This value gives a rough information about the actual core state.

From reflood analyses using the MAAP code the critical range for reflood starts above 1500 K peak core temperature (PCT) /9/. Since increased temperature rise occurs due to the onset of Zircaloy oxidation the time window between 1500 K and cladding failure temperature used in the S/R5 code (2350K) is rather small.

3.1.3 Secondary system

Simulation of the secondary system was maintained as used in normal accident analyses **/7/**. The maximum secondary side pressure is limited by steam generator (SG) safety valves to 9.15 MPa. A controlled secondary side depressurization with a 100 K/h cool-down rate to 6.0 MPa is initiated by the reactor safety system (RSS) if the primary pressure drops below 11 MPa. 1800s after reactor scram manual depressurization to 0.2 MPa is simulated by opening the SG valves. In the unmitigated LOOP steam generators are dried out since 6200s (103 min) so that the influence of the secondary side on reflood scenarios discussed here is negligible.

3.2 LOOP scenario, base case

From different scenarios investigated (s. Table 3.1) the Loss-of-offsite power (LOOP, s. /7/) scenario was selected to be representative for delayed reflood prior to onset of oxidation and core degradation /9/. For this scenario, a total loss of alternating current (medium- and high-voltage grid) and a loss of emergency power supply driven by the small and the large diesel generators is assumed. Only battery power is available for the reactor control and safety systems, also to activate valves. For the LOOP “base case” no operator interaction is assumed besides primary depressurization so that simulation proceeds into core degradation forming a molten pool with contact to the heavy reflector after 4.5 h (s. Figure 3.6). For the reflood study, however, it is assumed that electrical power supply for ECC pumps can be reestablished at least 3.8 h after reactor scram. In the following section a short overview of the base case is given since some data are required in section 4.

3.2.1 Thermohydraulic phase

In Figure 3.6 results of LOOP "base case" calculation is shown, starting 40 min after loss-of-off-site power. The sequence of phenomena is discussed in detail in /7/. At loss of power, the absorber rods immediately drop into the core, shutting down the reactor. Primary coolant pumps and main feed water coolant pumps slow down, forced convection ceases to cool the reactor. After 10 sec main coolant pump cease and several seconds later the turbine valve is closed, turbine bypass valve is assumed to remain closed, so that no heat can be transferred to the steam condensator directly. Then heat flux by natural convection from the primary system to the steam generators (SG) increases secondary system pressure up to the set point of safety valves at app. 9.1 MPa (s. Figure 3.6 d). This relatively safe state of natural circulation is maintained up to SG dry-out (s. Figure 3.6 c) at app. 100 min (1.7 h) keeping the primary system temperature at saturation temperature (s. Figure 3.6 b). After SG dry-out primary system pressure increases up to the set point of the first safety valve (s. Figure 3.6 d, valve opens at 17.6 MPa). After SG dry out, no possible 2nd side measure can affect primary side.

If the pressure drops below 16.6 MPa the safety valve closes and the cycle starts again, as can be seen in Figure 3.6 d. This cycling lasts up to 2.5 h until the core outlet vapor temperature exceeds a defined value so that primary side depressurization is initiated by opening the dedicated PZR valves (824+834). Reactor scram is triggered by the signal "system pressure low" starting 2nd side depressurization, as can be seen in Figure 3.6 d. App. 10 min after that initiation, primary system pressure has dropped below 4.5 MPa and the accumulator check valves open. Four minutes later, the accumulators are empty and the core is refilled as can be seen in Figure 3.6 c. 30 min after scram manual depressurization is simulated.

After blow-down and refill primary system, pressure sustains at app. 1.0 MPa according to the specified containment pressure of 0.2 MPa and the pressure losses along the flow path through hot leg, surge line, PZR, and depressurization valve. The boil-down period starts at app. 3.2 h with a collapsed water level of 4.5 m in the core. 3.3 h into the transient the core heat-up phase starts, the peak core temperature (PCT) rises with app. 0.45 K/s for 30 min up to 1300K. First hydrogen production is calculated at app. 3.7 h (13300s), within next 10 min (13950s) the peak core temperature exceeds 1500 K initiating the excessive hydrogen release with its first release peak at 14050s.

In this phase the evaporation rate varies between 24 kg/s steam mass flux at 3.3 h and 3 kg/s at app. 4 h (s. Figure 9.3 top). Therefore the collapsed water level in the core declines with app. – 0.2 cm/s at 4 h in the upper third of the core and app. 0.03 cm/s at the lower end as can be depicted from Figure 9.3 bottom. At 4.5 h the core is nearly completely empty, only water in the lower plenum remains.

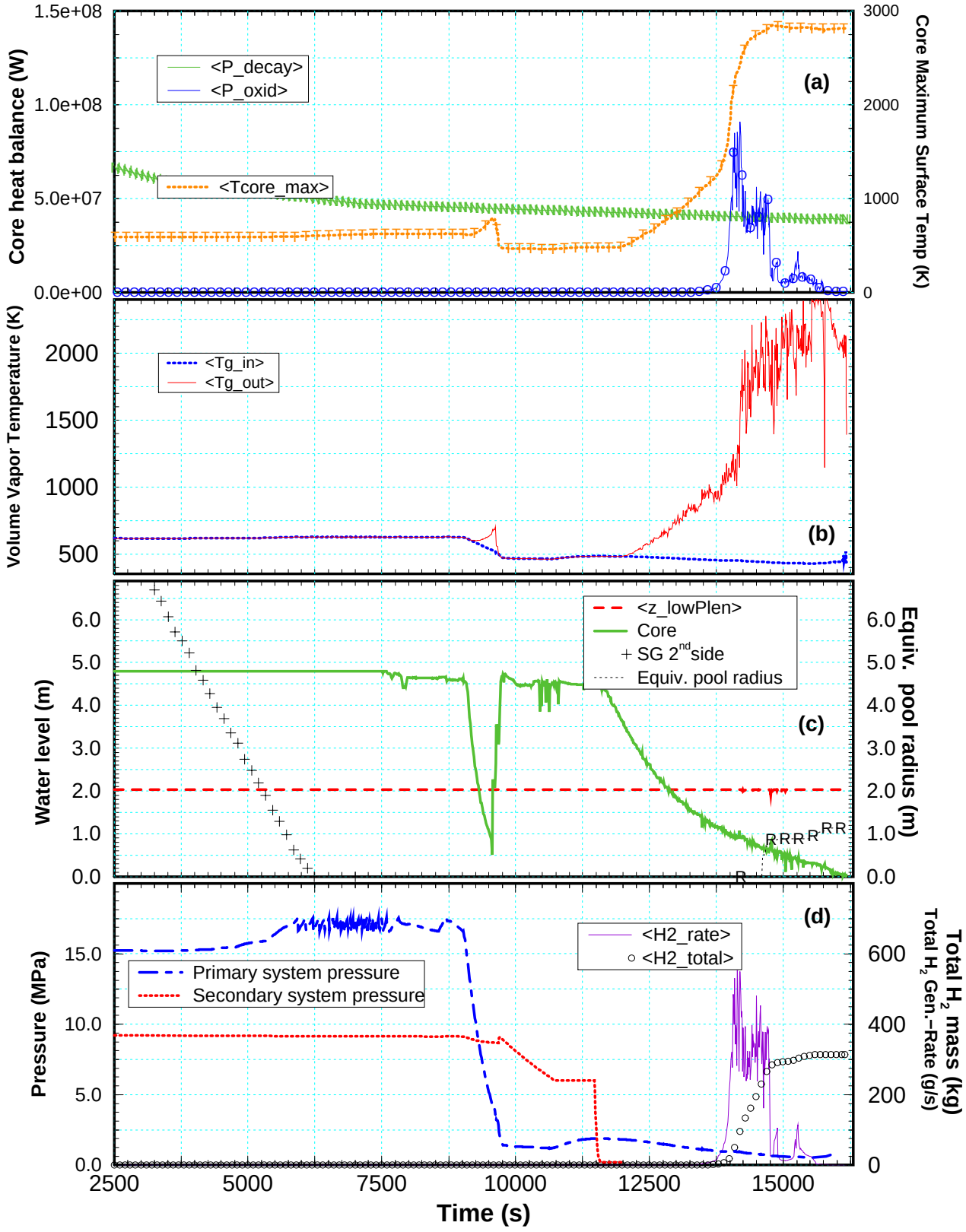

Figure 3.6 Results of LOOP ”base case” with S/R5m31: (a) nuclear and chemical power (left side) and PCT (right side), (b) core inlet and outlet gas temperatures, (c) collapsed water level of SG 2nd side, core and lower plenum and equivalent radius of a molten pool in the core, and (d) pressure history (left) and hydrogen production rate and total hydrogen mass (right).

3.2.2 Component failures

Clad ballooning and failure (breach) is calculated to occur in the four inner rings at 3.8h (13750 s) and in the outer ring at app. 5 min later. This can be explained due to the influence of the heavy reflector (HR) which acts as an efficient heat sink by radiation since the inner surface temperature is just above saturation temperature and, partly, by the radial power distribution (s. Table 3.2).

At 14003s, first absorber rod failure leading to melt relocation is calculated. The cladding of the fuel rod fails with subsequent melt release at 14105s in the 12^{th} axial node of the central ring, and metallic melt relocates as droplets into the 11^{th} axial node. Within the next three seconds the same process is calculated to happen in adjacent rings up to the 4^{th} ring. The fuel rod in the 5^{th} ring follows 10 s later.

3.2.3 Core degradation

At around 14095s the PCT reaches 2300K, the maximum reflood initiation temperature of this study. The core is only slightly damaged, limited melt relocations had occurred, so that S/R5 reflood models can be applied (s. section 2.2, and 2.3).

After 14950s a molten pool is formed in the center channel of the core spreading in radial direction and relocating downward. With formation of a molten pool thermohydraulic models for reflood are not longer applicable. In such a case 3-D models simulating thermohydraulics for porous debris states have to be used.

4 DETAILED RESULTS OF REFLOOD CALCULATIONS

4.1 Design base type reflood

In case of reflood during design basis accidents (DBA) no additional hydrogen, no melt relocation, and no debris formation influences the reflood process. So that primary system dynamics and thermal hydraulic behavior of the core can be analyzed effectively. In the fist case full availability of all ECC systems is assumed and the reflood is initiated at a PCT of 1300K to ensure clearly DBA conditions.

4.1.1 Thermohydraulics

Starting with LOOP "base case" conditions (s. section 3.2), the reflood initiation temperature of 1300 K is exceeded at 13800s. At ECC activation, both systems, the LHSI as well as the MHSI start to feed in (s. Figure 4.1 b), leading to a sudden rise of the collapsed water level in the vessel (c). The evaporating water leads to a steep increase in vapor production in the lower half of the core. The produced steam as well as pressure losses caused by the increased mass flow rate through surge line and PZR valves increase primary system pressure calculated for the upper plenum as shown in Figure 4.1 a. App. 30 s later, the rising system pressure exceeds the set point of the LHSI system which ceases to inject for more than 70 s. The MHSI is only slightly influenced and continues to refill the core. Secondary system pressure remains at containment pressure level (s. Figure 4.1a).

At 13800 s the collapsed water level in the vessel is app. 2.5 m (s. Figure 4.1 c), indicating a collapsed water level in the core of app. 1.2 m. The fuel rod cladding temperatures (s. Figure 4.2) are less than 900 K in the lower half of the core and the axial temperature profile is rather flat (s. Figure 5.7 top). The calculated dip in the collapsed water level of the vessel at 13810s (s. Figure 4.1 c) is affected by vapor coming from the downcomer (DC) and the cold leg piping. The vapor injected into the core prior to injection of cold water from the ECC system expels water into the upper plenum so that less water mass remains in core and lower plenum for a short time period. This behavior can be observed in all reflood calculations either if all ECC are activated or, more pronounced, by only one MHSI and one LHSI system become available on request.

At 13940 s core collapsed water level reaches the hot leg level, feeding water into the main coolant piping system and into the pressurizer (PZR) (s. Figure 4.1 d). This leads to mass flow spikes when liquid water flows to the steam generators. The behavior is less pronounced in the triple loop since the PZR is connected to the single loop. Between 13860s and 13950s water flows back from the pressurizer due to pressure drop in the core affected by cooling effects and increased pressure losses in the PZR valves due to a reduced void. At around 14250s the primary system and the PZR are filled completely and the reflood is terminated. The slight pressure increase after 14200s is due to saturated water passing safety valves and increasing pressure loss.

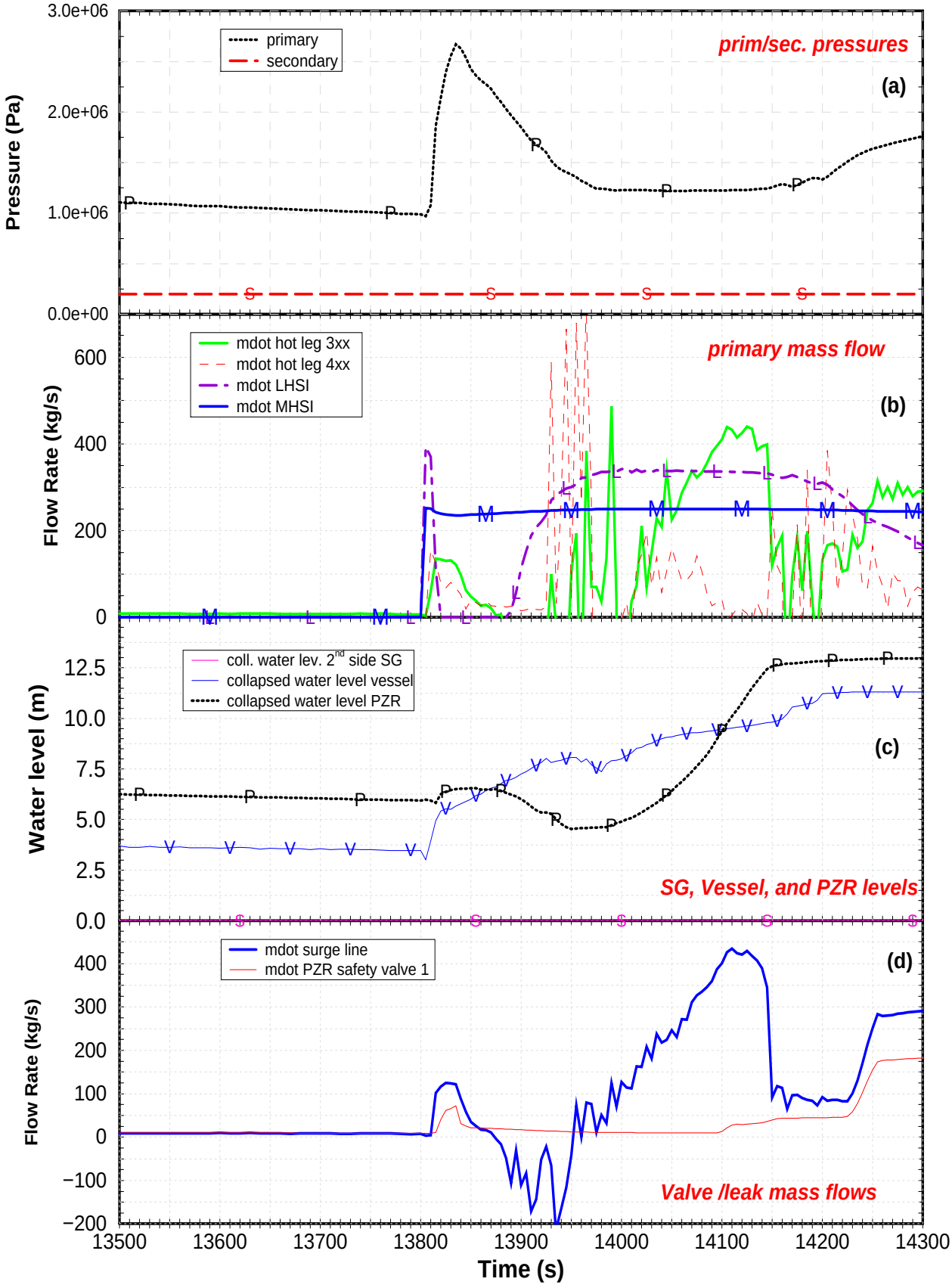

Figure 4.1 Thermal hydraulic conditions during reflood initiated at PCT 1300K using all ECC systems: (a) system pressure, (b) ECC and hot leg mass flow rates, (c) collapsed water levels, and (d) mass flow rates through surge line and PZR safety valve.

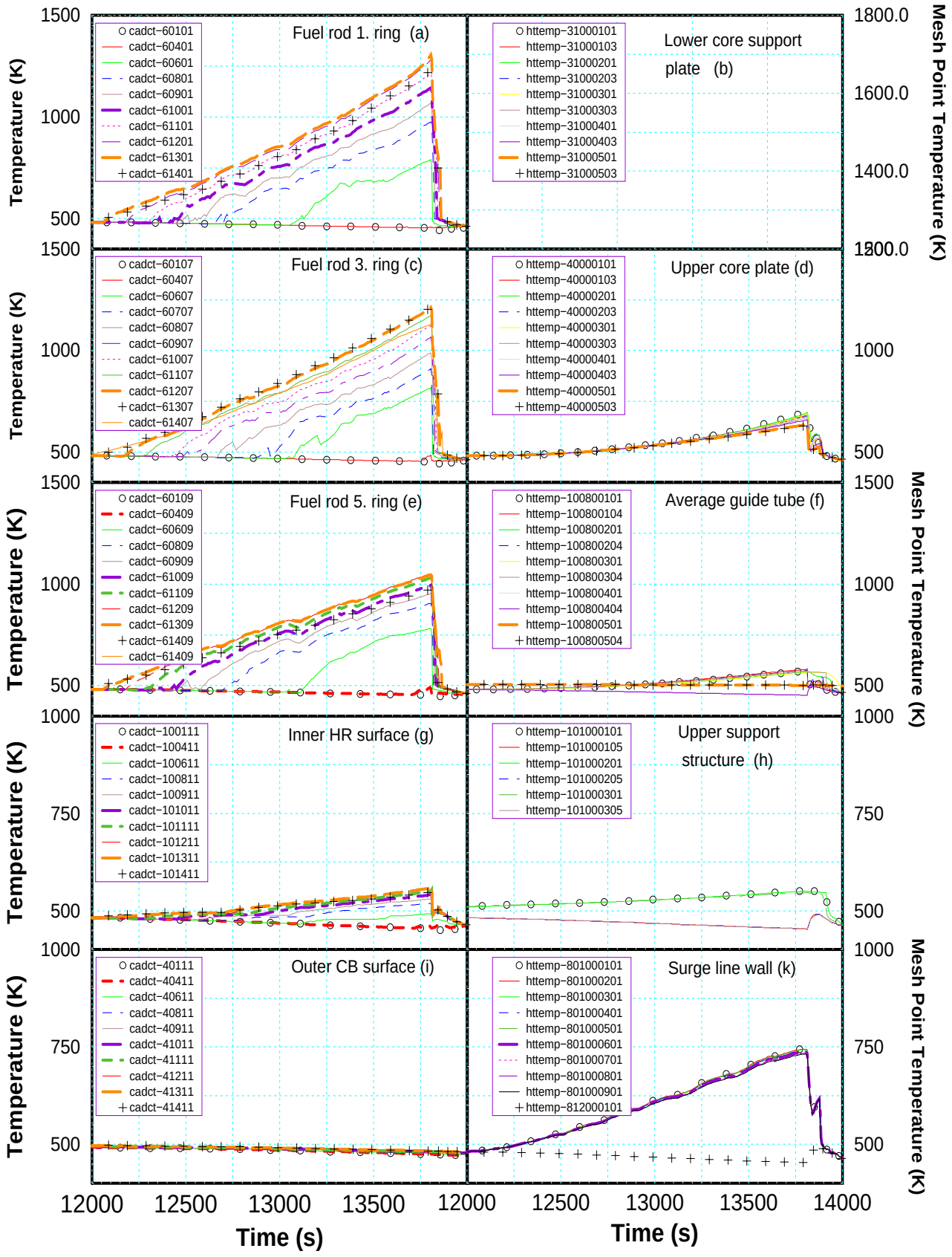

Figure 4.2 Structure surface temperatures calculated for a reflood initiation temperature of 1300K prior to and during reflood, left side: inside and around the core, right side: in lower/upper plenum and in the surge line.

4.1.2 Temperature history

On the left of Figure 4.2 temperatures are shown for fuel rods, HR inner surface, and CB outer surface. On the right side temperatures calculated for vessel internals such as lower / upper core plate, upper support structure, and support columns (s. Figure 3.1) as well as wall temperatures along the surge line (k).

Generally, the core is calculated to cool-down as designed in the DBA assuming normal ECC operation. In the inner four rings Figure 4.2 (a), (c), the temperatures are similar, the fifths ring is several hundred Kelvin colder due to the cooling effect of the HR (s. Figure 4.2 (g)). The HR and CB are near or at saturation temperature (s. Figure 4.2 (i)). The fuel rod behavior during boil down can be seen in (a), (c) and (e) the heat-up rate in different levels is nearly the same indicating that no additional energy from a zirconium steam reaction is released. The wall temperatures of surge line given in Figure 4.2 (k) have been calculate to app. 750 K, mainly due to evaporated steam.

4.2 Reflood initiation below 2000 K

At the reflood initiation temperature of 1700 K first temperature escalation was calculated and an increased hydrogen production. Therefore, these results will be discussed in more detail, comparing results of the 1700 K case and the 1900 K case. In section 4.3 the 2100 K and the 2300 K cases (s. Section 4.3) will be discussed and in section 5 a comparison and discussion of all results will complete the evaluation.

As mentioned above, below 1700 K PCT conditions can be handled by DBA code systems easily, since no noticeable oxidation and melt relocation is calculated to take place. In the following, influence of the assumed availability of ECC systems will be emphasized in order to investigate the influence of the time period at high temperature to progressive core damage.

4.2.1 All ECC systems

Figure 4.3 gives an overview of the two reflood cases 1700K and 1900K. In case of 1700K, the system pressure drops at around 14100s below the set point of the LHSI systems. At that time, however, the calculation states that the core has already been refilled (Figure 4.3 center). Due to the higher system pressure increase in the 1900K case the MHSI pump injection rate is slightly lower than in the 1700K case. The difference of 0.8 MPa in the maximum system pressure shown in Figure 4.3 top is a result of enhanced hydrogen release and additional steam production. The calculated hydrogen production for the 1700K case does not show a significant release prior to quenching (s. Figure 4.3 bottom) whereas in the 1900K case the release rate increases up to 4 kg/s. Within 100s more than 50 kg of H_2 are released.

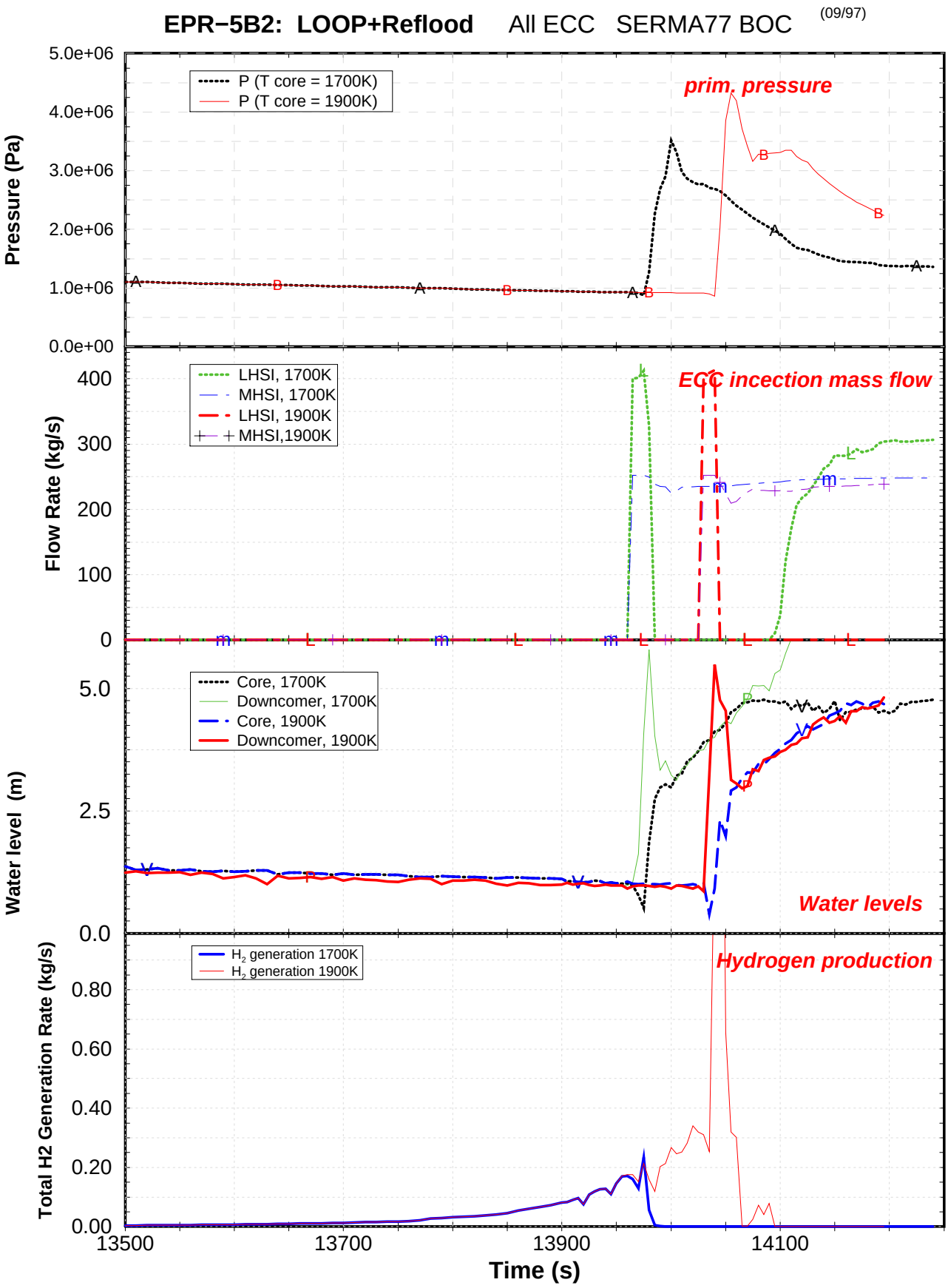

Figure 4.3 Thermohydraulics and hydrogen production rate for the scenario “All ECC systems” and cases 1700 K and 1900K: (a) primary system pressure, (b) ECC injection rates, (c) collapsed water level, and (d) hydrogen production rate.

For the 1700K cases the temperature history resembles that shown in Figure 4.2 for the 1300 K. No melt relocation and no blockage formation were calculated so that intact fuel geometry can be assumed up to safe core state, since clad ballooning only slightly influences the net fluid channel cross section (< 8%).

In the 1900K case zones in which shattering or even metallic melt relocation was calculated show temperature increases (s. right side of Figure 4.5). Time scales for initiation of reflood, first melt relocation, and local shattering are summarized in Table 5.1. The time window in which the upper part of the core remains at temperatures above initiation temperature is rather short (app. 30s) so that no severe core damage was calculated. Metallic melt relocations were stopped by the rising water level. For comparison the peak core temperature (PCT) of all reflood calculations are summarized in Figure 5.3 and Figure 5.5.

4.2.2 One of each kind

In Figure 4.4 thermohydraulic conditions for the 1700K and 1900K case with only one ECC system of each kind (1 MHSI + 1 LHSI) are shown. These cases are worse case scenarios because they represent minimum reflood capability which can be assumed realistically. In reality, however, if electric power supply can be reestablished all ECC systems will be available or not-available due to common cause errors.

At a first glance no significant differences can be seen compared to the cases discussed above (s. Section 4.2.1) using Figure 4.3. Naturally injected water masses are only ¼ so that the time scales are extended as can be depicted from comparing Table 5.2 with Table 5.1.

In the 1700K case the pressure is app. 1.0 MPa less compared to the 1900K case mainly due to less produced hydrogen (s. Figure 4.4 top). The core refill is completed app. 400s after initiation accelerated by the regaining reflood capacity of the LHSI system (s. Figure 4.4 center). Additional hydrogen release is also calculated to be 25 % higher compared to the case “All ECC activated” (s. Figure 4.4 bottom), however, oxidation ceased when LHSI systems continued to feed in.

In the 1900K case the first oxidation comes together with first metallic melt relocation (s. Figure 5.2) in the axial zones 10 to 13 (core level 2.8m – 3.8m). Due to the low oxide scales prior to reflood (s. Figure 5.7 bottom) shattering conditions are calculated to occur at 14096s, app. 40 s after first temperature spike (s. Figure 4.5 a-b). The outermost ring remains cold up to 14150s. The lower half of the core is quenched as foreseen due to the high reflood rates supplied by the LHSI system. Oxidation and smooth rise of core water level continues as long as shattering criteria are reached in the inner rings (s. Table 5.2).

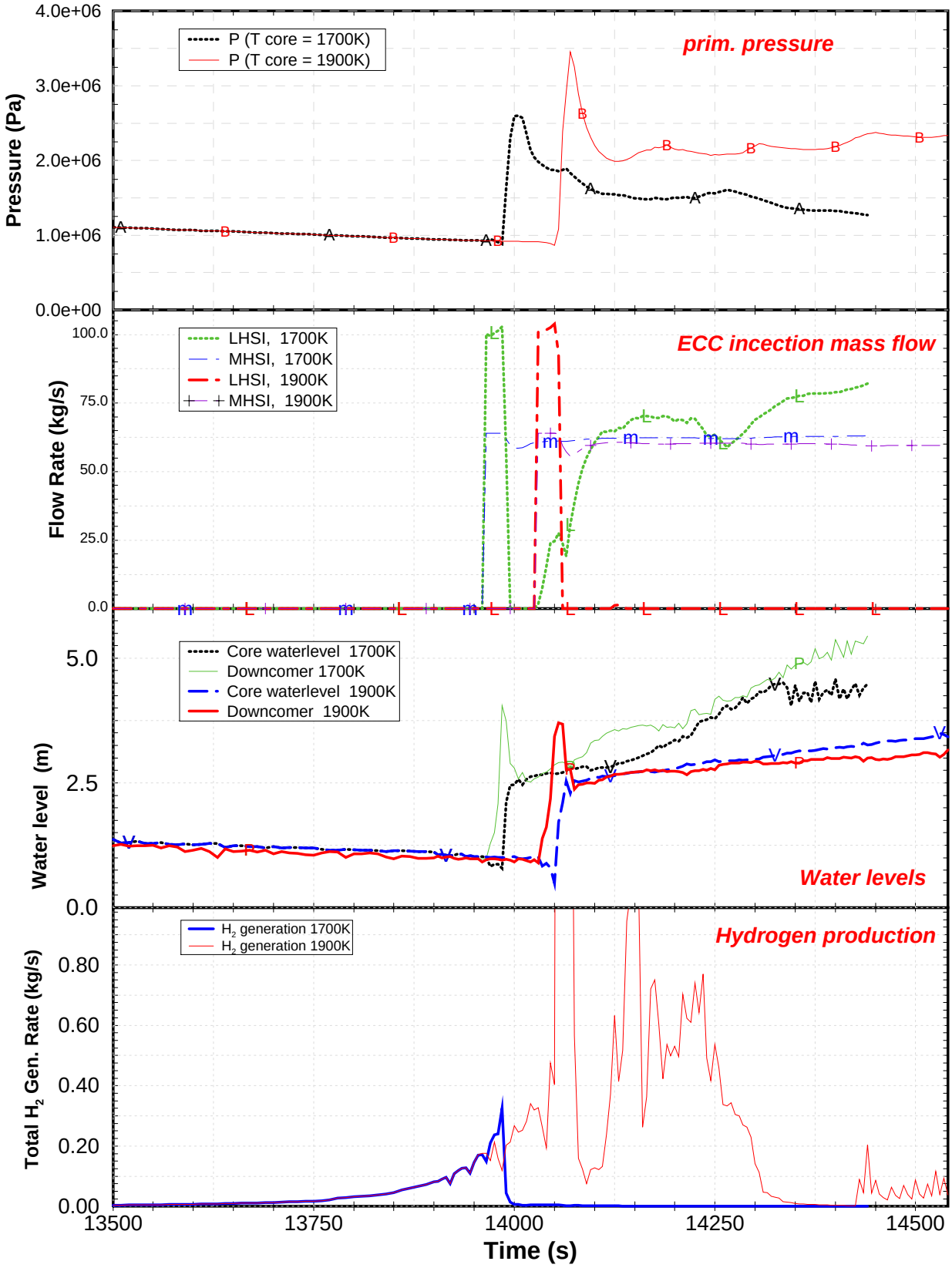

Figure 4.4 Thermohydraulics and hydrogen production rate for the scenario “1 MHSI + 1 LHSI “ and cases 1700 K and 1900K: (a) primary system pressure, (b) ECC injection rates, (c) collapsed water level, and (d) hydrogen production rate.

After ceasing of the LHSI, convective heat transfer is reduced and radiative heat transfer from inner rings plus exothermal energy starts a secondary heat up. This leads to conditions where shattering can be calculated. At 14426s (s. Table 5.2) short time cool-down triggers shattering in the outer ring but due to sufficient cooling (radiation to the HR) the temperature shows only a smooth increase. At app. 14560s the calculation was stopped when the PCT, actually localized in the fifth ring top axial zone, decreases below 1500K and the calculation predicts safe core state.

The total hydrogen mass is app. three times as high as in the 1900K case with all ECC systems whereas the maximum hydrogen production rate is only twice as high. Here the very low reflood rates allow oxidation for rather long times until PCT drops below 1500K. Also peak hydrogen release rates only occur during the initial reflood phase where both systems feed in.

Temperatures development in the upper plenum structures reflect the enhanced convective heat transfer since no radiative heat transfer has to be considered due to steam and 2-phase fluid in the coolant channels. Therefore temperatures increase up to the end of the calculation but they remain far below structures melting point (app. 1700K).

In Figure 4.5 the differences of both ECC injection cases become obvious for the 1900 K case, comparing the temperature history for 1 MHSI + 1 LHSI (left) with those for All ECC systems (right). Two stages can be clearly separated: a rapid instantaneous temperature rise at reflood initiation time (s. Figure 4.5 a + c) and a delayed temperature escalation app. 60 s later. Such stages are not observed in the second case (“All ECC available”) where only a sharp but less high temperature increase occurred. In both cases melting of the upper grid spacer at app. 3.5 m triggers cladding perforation and release of molten Zircaloy because no protective oxide scale could have been formed there. Presently it cannot be excluded that the delay time for Zry-Ni interaction found in separate effects tests is not appropriate for this transient case. The temperature increases due to relocating melt triggering oxidation in the axial zones below.

In both cases reflood is initiated at 14028s and first temperature escalation is observed at 14042s in case of All ECC systems (see: @ in Table 5.1) and 10s later if only 1 MHSI + 1 LHSI feed in (see: @ in Table 5.2). This time delay is mainly due to the flooding of pipes and the downcomer. No melt relocation is observed in the All ECC systems case whereas at 14065s droplet type melt relocation was calculated.

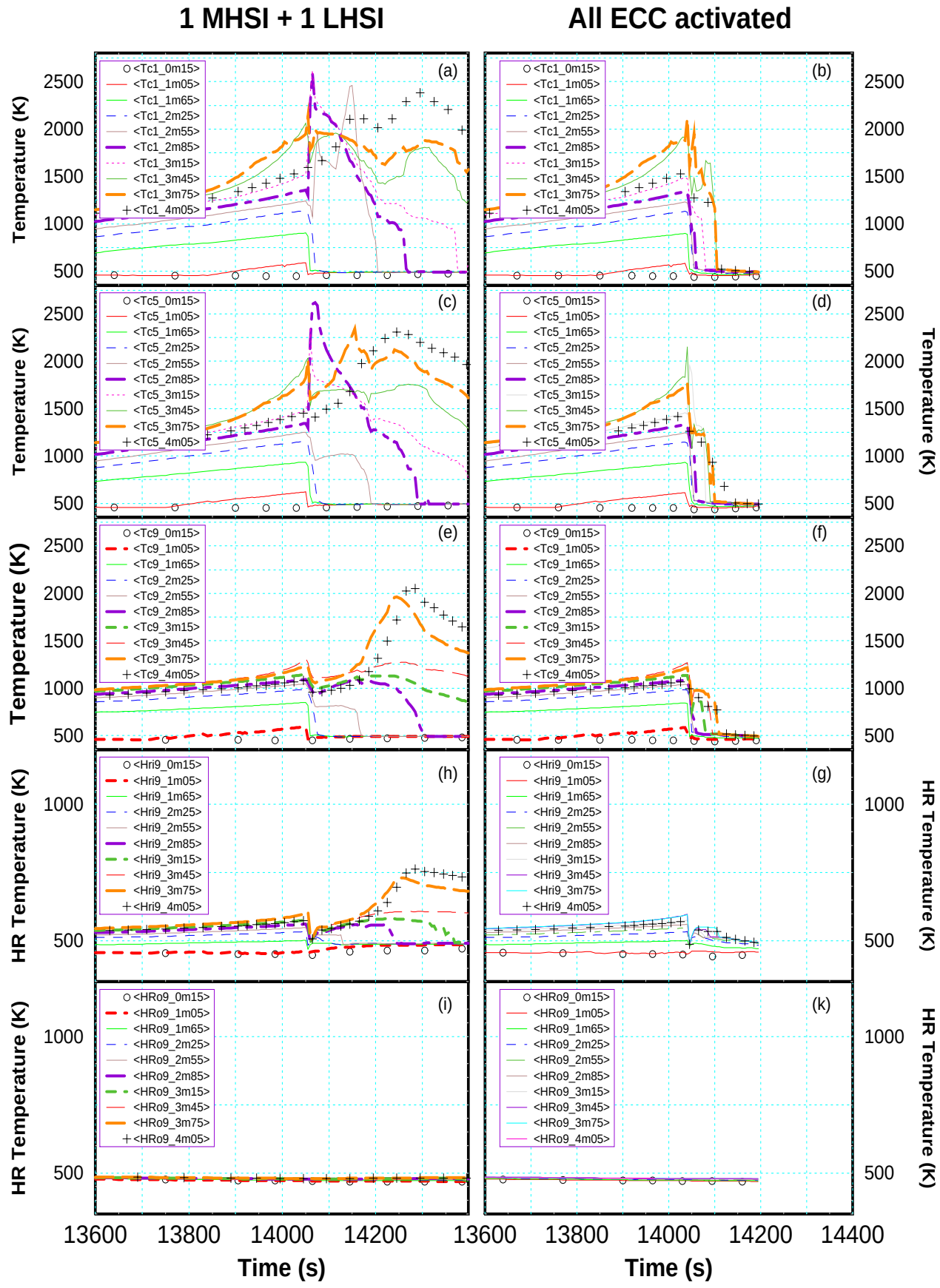

Figure 4.5 Temperature history in core and HR for the scenarios: “1 MHSI + 1 LHSI” (left side) and “All ECC systems” (right side) for 1900K reflood initiation temperature

4.3 Reflood initiation beyond 2000K

Beyond 2000K metallic part of the cladding (β-Zry) becomes liquid but remains kept within the oxide shell. In case of shattering a steep cool-down to 1500K has to be calculated for the thick ZrO_2 layer (s. section 2.2). The liquid metal freezes and oxidizes subsequently, if no fuel cladding interaction has been calculated before. If this is not the case, shattering will not be calculated, since no β-Zry would remain. Core degradation will be discussed in detail in Section 5.1.

4.3.1 All ECC systems

From the thermohydraulic point of view system response calculated for injection of all ECC pumps resembles that discussed earlier in Section 4.2.1, except for the time delay due to higher reflood initiation temperatures. Most important difference is that the primary system pressure (s. Figure 4.6 a) stays for more than 100s at 3.5 MPa and 4 MPa respectively and only slowly decreases afterwards so that the system pressure remains above 2 MPa up to time of core refill (app. 240s later). At 14200s saturation temperature level is achieved in the whole core (s. Figure 4.7 and Figure 4.8). Again the LHSI (s. Figure 4.6 center) only feed in for app. 20s and ceased due to increasing system pressure and the four MHSI systems succeeded in flooding the core with an average speed of 1.5 cm/s.

Time window for severe core degradation is less than 70s for the 2100K and about 90s for the 2300K case, during which app. 100 kg hydrogen is released with a peak value of app. 8 kg/s. Also melt relocations take place as discussed in Section 5.1.1. Shattering only effects the inner three rings (s. Section 5.1.1) where only the upper 3-4 nodes experience temperature increase as shown in Figure 4.7 a-c. The outer ring remains rather cold with PCT of less than 1300K. Except for the zones where shattering is calculated the general tendency is rapid cool-down by steam and two phase fluid. Fuel rod quenching occurs at elevations of or just below collapsed water level indicating a strong droplet entrainment.

The high energy release due to the unlimited oxidation just after shattering cannot be compensated by heat transfer mechanisms to the fluid so that the temperatures rise with more than 70 K/s. Strictly speaking, conditions of the models in the severe accident codes rely on quasi steady state conditions, and this is not longer maintained in such extreme transient cases. For accident analyses, however, the predictions can be seen as upper limits of system behavior and hydrogen release especially with respect to the relatively coarse representation of the fragmentation process by the shattering model.

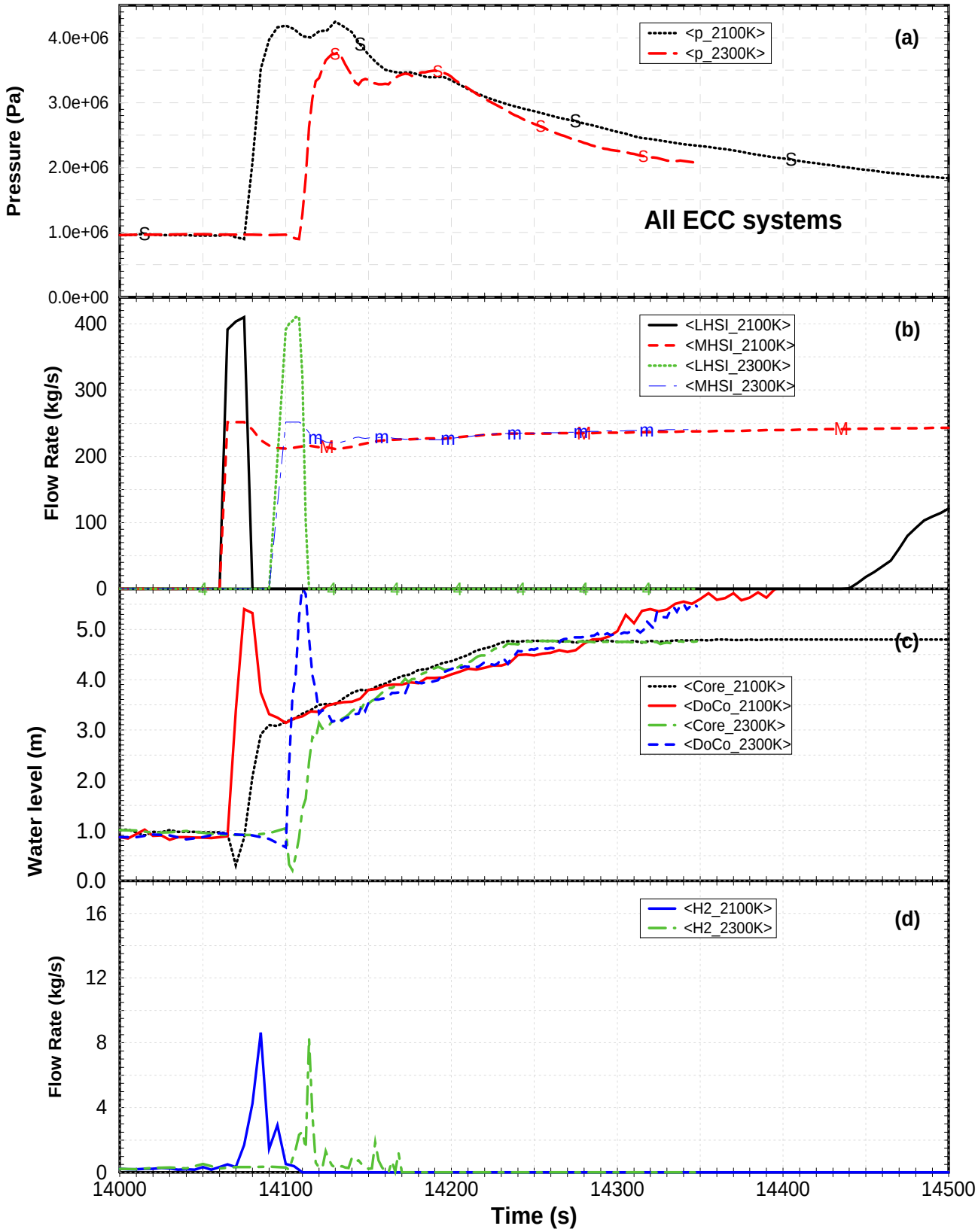

Figure 4.6 Thermohydraulics and hydrogen production for scenario " All ECC systems" and the cases 2100K and 2300K: (a) primary system pressure, (b) ECC injection rates, (c) collapsed water level, and (d) hydrogen production rate.

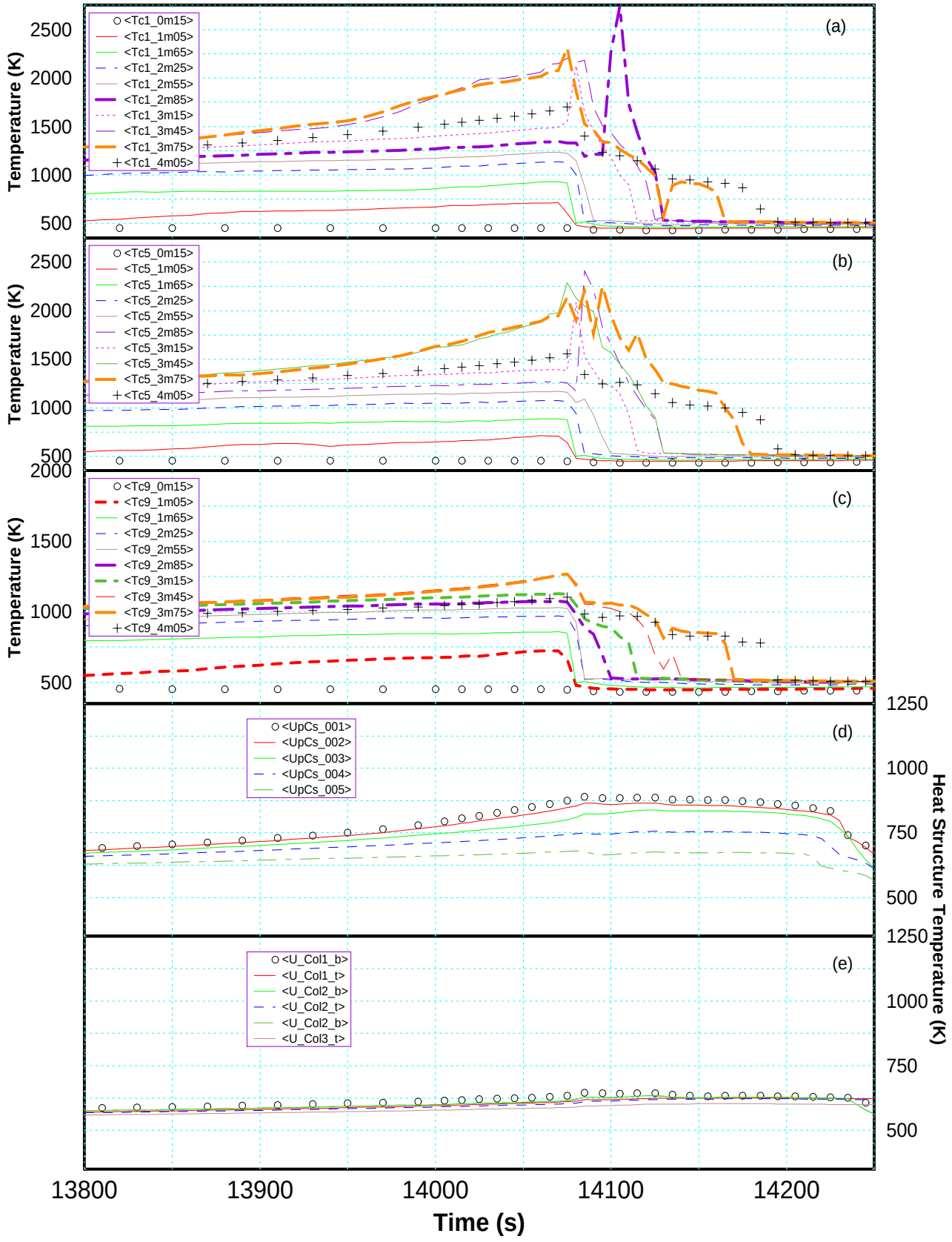

Figure 4.7 Calculated temperatures for the scenario “All ECC systems” at reflood initiation temperature of 2100K: (a) center ring fuel rod temperatures, (b) average ring fuel rod temperatures, (c) outer ring fuel rod temperatures, (d) upper core support plate, and (e) support columns in upper plenum.

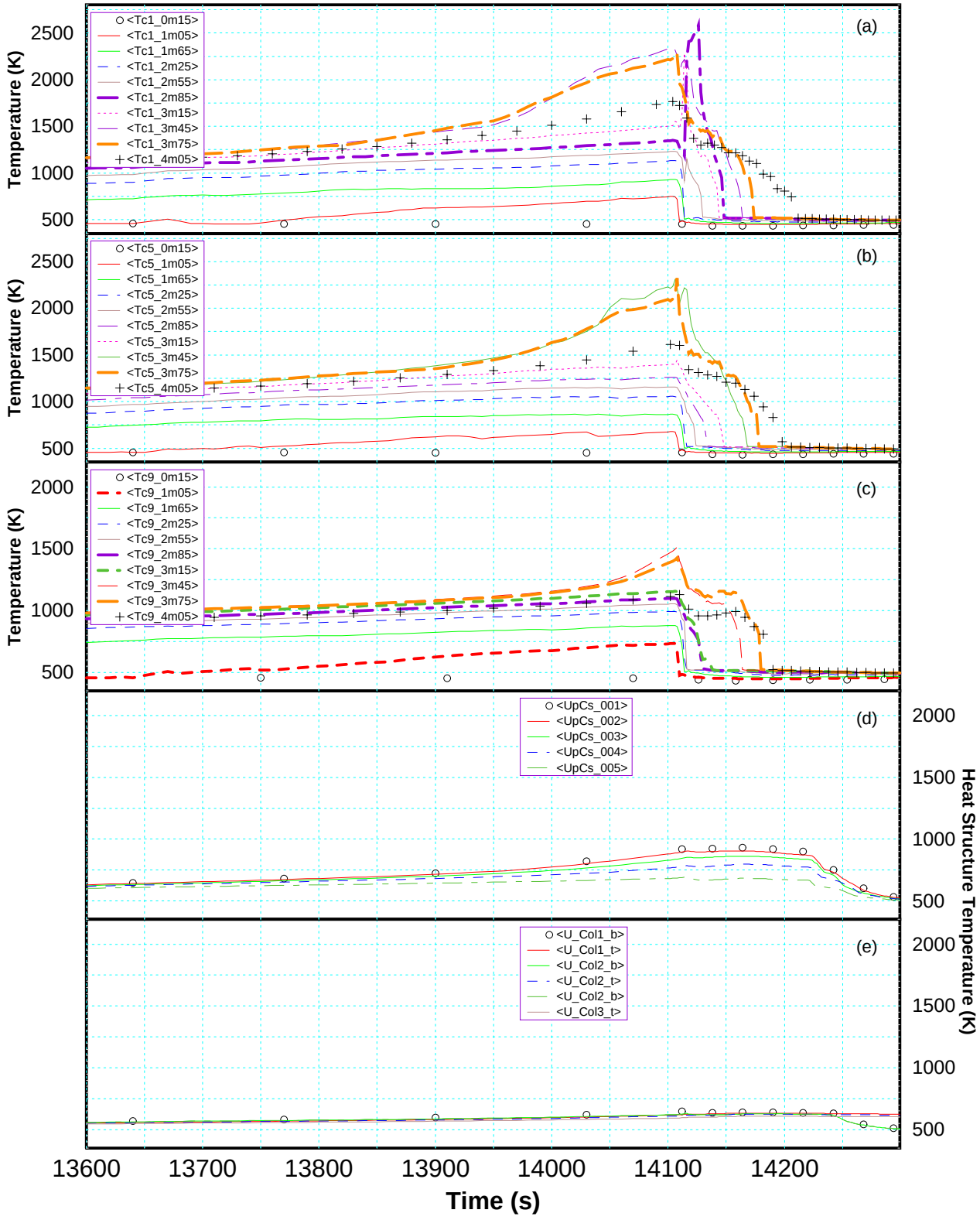

Figure 4.8 Calculated temperatures for the scenario “All ECC systems” at reflood initiation temperature of 2300K: (a) center ring fuel rod temperatures, (b) average ring fuel rod temperatures, (c) outer ring fuel rod temperatures, (d) upper core support plate, and (e) support columns in upper plenum.

Upper plenum structures remain cold as mentioned before. The upper core plate temperature remains below 870K in the 2100K case and below 900K in the 2300K case. The representative upper columns temperature remains below 800 K for both cases. Quenching is not calculated, the slope of calculated temperatures resembles more a smooth cool-down (< 10K/s) to saturation temperature app. 50s after core quench. This is more pronounced in the 2300K case given in Figure 4.8.

In all cases discussed here, the fuel rod temperature does not exceed the eutectic temperature of the UO_2-ZrO_2 system, so that no massive debris formation was calculated, however, the safety margin to this temperature is rather small. Here the conservative approach, the complete removal of all protective ZrO_2-scales may trigger unrealistic core degradation paths which become dominant in the late phase of in-vessel core degradation.

4.3.2 One of each kind

At last the extreme case late reflood initiation and low reflood rate is discussed. The system pressure rise is limited to 3.0 MPa (s. Figure 4.9), drops lightly below 2.0 MPa after ceasing of the LHSI pumps, increases to 2.2 MPa, and remains at that level until the end of the calculation. For a short period of 50s the LHSI pump feed in with a small injection rate, but no effect was observed with respect to the flooding rate. Within the next 300s the MHSI system is not able to refill the core, the upper two axial zones are not rewetted.

In the 2100K the highest hydrogen production rate was calculated (s. Figure 4.9) to amount to app. 16 kg/s. In the 2300K case the production rate is decreased mainly due to ongoing oxidation before reflood and shattering. Formation of metallic blockages prior to reflood initiation is not calculated due to the oxide layer failure criteria which was set to 2350K.

Generally in both cases the origin of the calculated reaction it is not quite clear. During boil-down the oxidation is controlled by the availability of steam within the core. If steam becomes excessive the oxidation will be unlimited (only limited by metal available). From the event sequences and the temperatures and hydrogen data, the hydrogen production starts prior to initial shattering, triggered by metallic melt relocation. Nevertheless, steep temperature increase is calculated starting at 14095s in 2.85m while the first shattering event is stated at 14106s at app. 3.15 m core elevation.

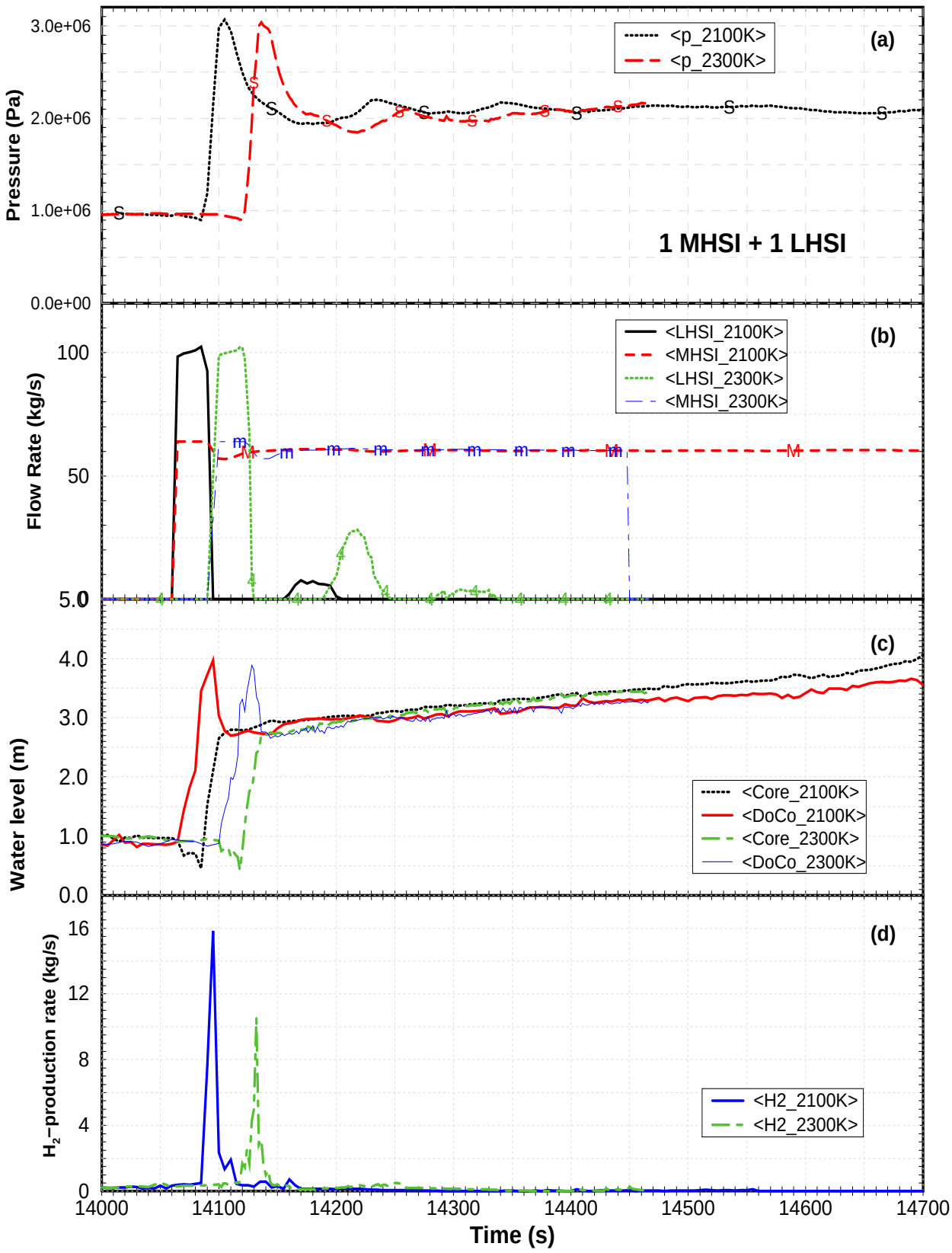

Figure 4.9 Thermohydraulics and hydrogen production for scenario " 1MHSI + 1 LHSI system" and the cases 2100K and 2300K: (a) primary system pressure, (b) ECC injection rates, (c) collapsed water level, and (d) hydrogen production rate.

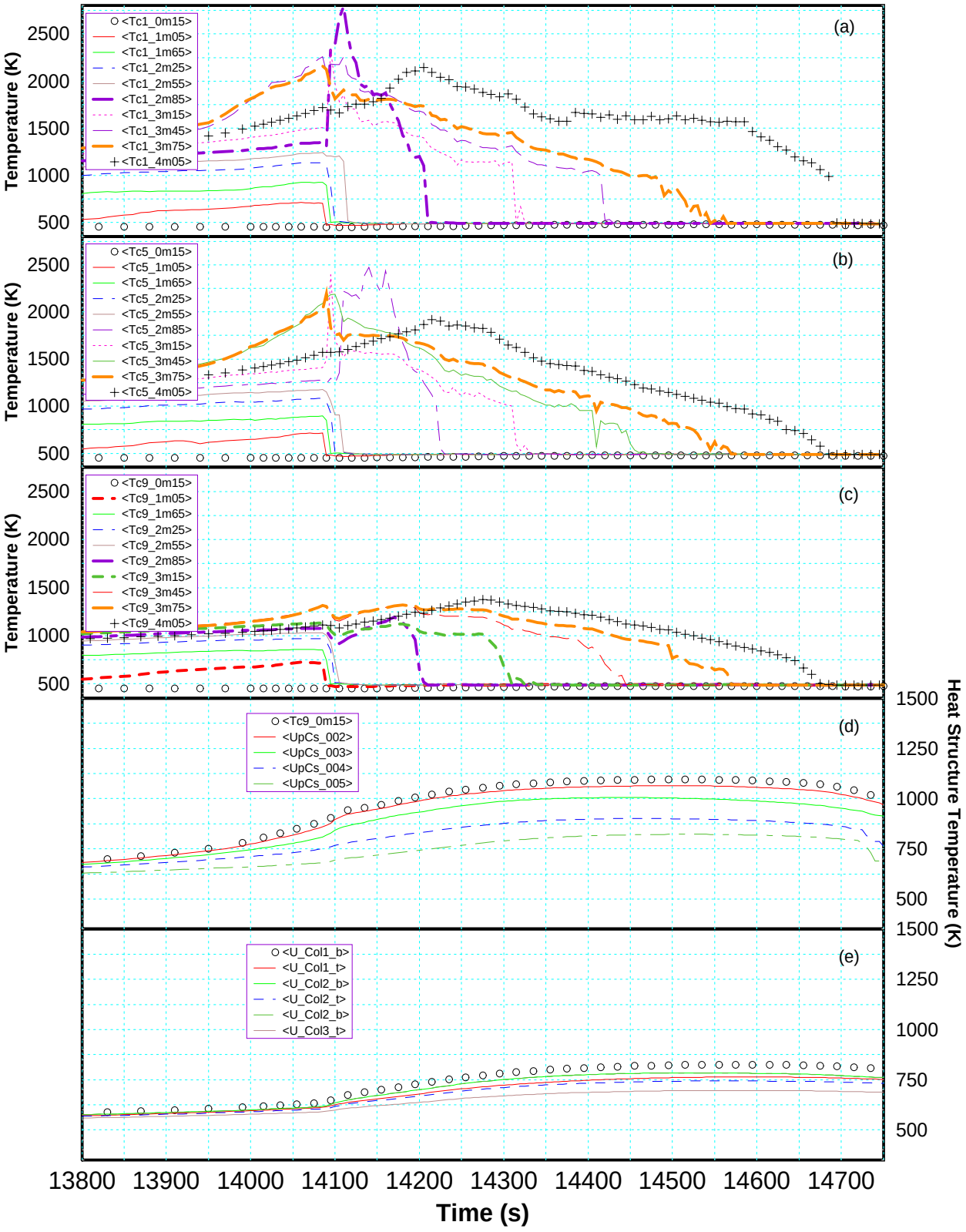

Figure 4.10 Calculated temperatures for the scenario “1 MHSI + 1 LHSI system” at reflood initiation temperature of 2100K: (a) center ring fuel rod temperatures, (b) average ring fuel rod temperatures, (c) outer ring fuel rod temperatures, (d) upper core support plate, and (e) support columns in upper plenum.

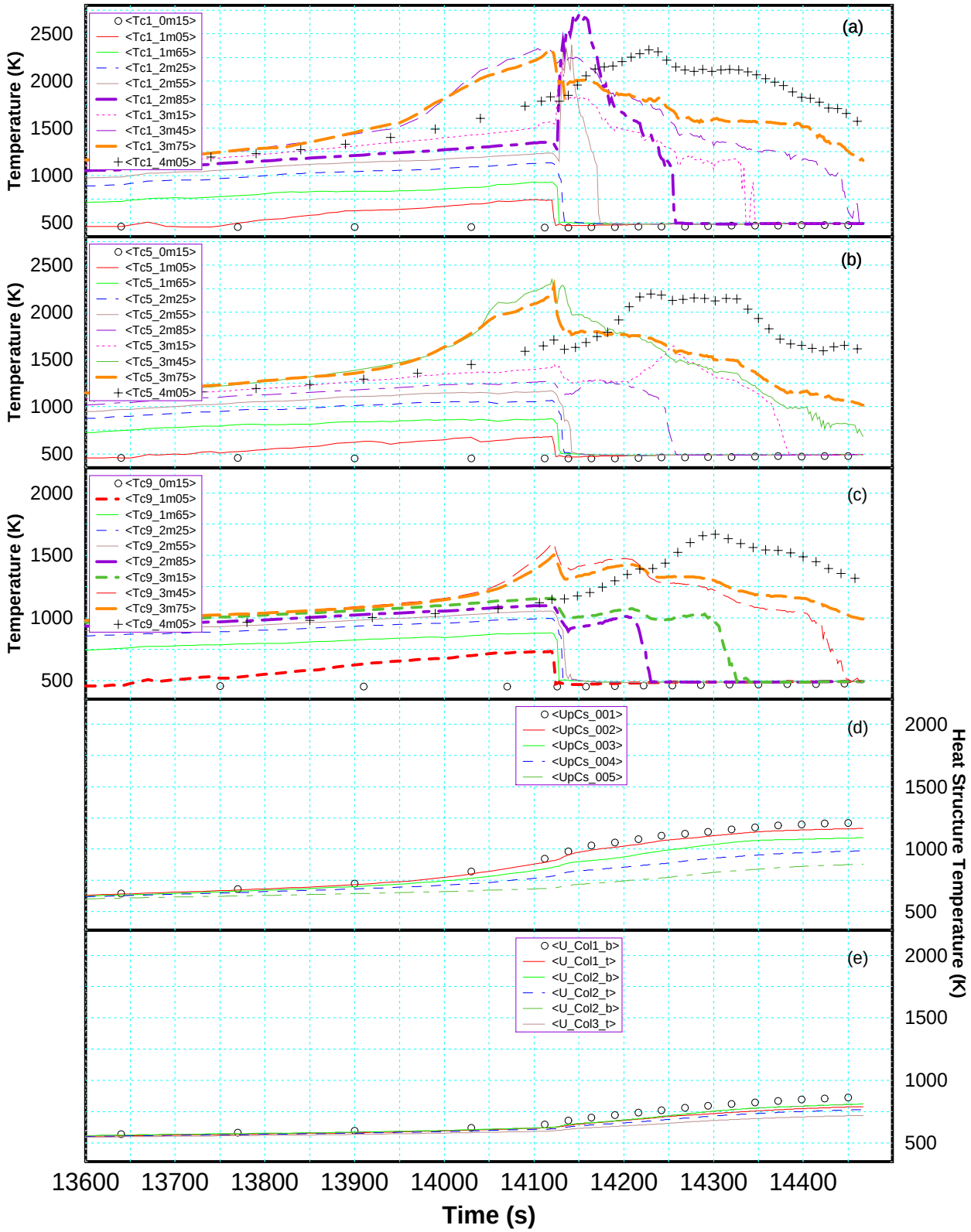

Figure 4.11 Calculated temperatures for the scenario “1 MHSI + 1 LHSI system” at reflood initiation temperature of 2300K: (a) center ring fuel rod temperatures, (b) average ring fuel rod temperatures, (c) outer ring fuel rod temperatures, (d) upper core support plate, and (e) support columns in upper plenum.

5 SUMMARY OF RESULTS

The study includes calculations of the base case, the LOOP without reflood, as well as ten LOOP scenarios with reflood initiated at 1300K, 1500K, 1700K, 1900K, 2100K, and 2300K. In each of the last four cases reflood water is injected by activation of either all ECC or only one of each kind (1 MHSI + 1 LHSI). Results were analyzed with respect to:

- Influence of modeled material relocation on the sequence of phenomena (section 5.1)
- Efficiency of mitigation measures in case of delayed reflood situations for the EPR (section 5.2)
- Definition of reactor conditions to be simulated in the FZK QUENCH facility (section 5.3).

5.1 Core degradation

As stated earlier neither significant oxidation nor core degradation events were calculated below and at 1700 K. So discussion is restricted to six cases shown in Table 5.1 and Table 5.2. Here, time and location inside the core are given for fuel rod shattering and absorber rod melt release and relocation. Also in the fist column, time of reflood initiation (init:), time of refill of the 3rd axial zone (@) which corresponds to an elevation between 0.9 and 1.2m in the active core, first calculated metallic melt (t_{first}), and the axial zone of relocation are indicated. The 3rd zone is the lowest dried out zone prior to reflood initiation.

Generally the use of the code is restricted to intact fuel rod geometry. In case of blockages only the reduced hydraulic diameter is taken into account, but neither unsymmetrical shape and geometry of the coolant channel nor the influence of increased surface roughness are considered. So from that time calculation become uncertain since surface roughness, shape, and area of the effective coolant channel cross-section influences flow condition and hence wall heat transfer coefficients. If only absorber melt is calculated to relocate this influence can be neglected for this study because the relocated melt mass is rather low and, due to the low melting temperature is relocates to lower elevations. However, if melt relocation is not restricted to a minor part of the core cross section, the global prediction of the reflood process is disturbed because of non-validated conditions.

As known from integral tests, blockages generally hinder water level rise locally but enhance droplet entrainment leading to strong carry-over effects. Due to these uncertainties detailed discussion is restricted to conditions prior to blockage formation. Also an extension of the study to higher reflood initiation temperature will increase the problem to separate between physical sound results and artificial effects due to unknown and not reliably simulated conditions in the fluid channel. Presently there exists a knowledge gap between flooding of intact fuel rod elements as investigated in the DBA analyses and flooding of debris beds investigated for in-vessel late phase core degradation.

5.1.1 All ECC systems

In case of Q4 ("All ECC systems") the reflood time is rather short (less 2 min) and the enhanced oxidation triggered by shattering is restricted to the inner three rings except for the 2300K case, where shattering starts in the fourth ring. This is due to the ongoing oxidation prior to reflood initiation in combination with the shattering conditions (s. Section 2.2). In these cases no shattering and no absorber damage is calculated in the outermost ring due to radiation and convective heat transfer to the HR. Results also reflect the strong dependence on shattering criteria as can be seen in the results calculated for the 2300K case.

Table 5.1 List of events for the cases: "All ECC systems" with respect to: initiated oxidation, "shattering" and absorber rod failure as a function of time, axial, and radial position

Case **Q4**		Time (sec)	**Fuel rod** Shattering					Time (sec)	**Absorber rod** Failure and melt release				
T (K)	***t (sec)***	***Ring***	***1***	***2***	***3***	***4***	***5***	***Ring***	***1***	***2***	***3***	***4***	***5***
1700			---	---	---	---	---		---	---	---	---	---
		Ring	1	2	3	4	5	Ring	1	2	3	4	5
1900		14044		12	12			14003		13/14			
Init:	14028	14046	13	13				14012	12				
@	14042	14052		11	11			14014			13/14		
.t first	---							14017		12	12		
		Ring	***1***	***2***	***3***	***4***	***5***	***Ring***	***1***	***2***	***3***	***4***	***5***
2100		14084	13	13	13/11			14003	12				
Init:	14062	14086	11	11				14008		13/14			
@	14076	14092	12	12				14011		12			
.t first	14078	14100			12			14017			13/14		
Zone	9	14102			10			14031			12		
		14107		10				14089	11				
		14113	10										
		Ring	***1***	***2***	***3***	***4***	***5***	***Ring***	***1***	***2***	***3***	***4***	***5***
2300		14111				12		14003	12				
Init:	14095	14116				13		14008		13/14			
@	14108	14117	13	13	13			14011		12			
.t first	14111	14119	11					14017			13/14		
Zone	9	14131	10	12	12			14031			12		
		14133	12					14089	11				
								14104				12/14	

Calculated shattering and absorber rod failure is restricted to an axial core segment between 3.0 m and 3.8 m, far above the initial water level. By absorber rod failure the Ag-In-Cd melt in the 14th level is released in the 13th node. In radial direction the absorber rod failure is also restricted to the inner four rings. Temperature increase due to oxidation leads to fuel clad interaction so that in all three cases material relocations were calculated to occur in the axial core levels mentioned above (s. Figure 5.1).

On the left side the accumulated UO_2 masses and on the right side the corresponding Zry masses in each axial core zone are given. In case 1900K only two axial zones (12, 13) failed just after reflood initiation, relocating app. 100 kg U-Zr-O melt into the 11^{th} axial zone. Similar behavior is found for the 2100K case, however, three axial zones (11-13) failed within 30s after reflood initiation forming a blockage in the 10^{th} zone (app. 3.0 m) 500 kg U-Zr-O and a metallic melt in the 9^{th} axial zone with app. 800 kg Zry, which is partially oxidized. The same happened in the 2300K case, with 1000 kg U-Zr-O in the 10^{th} axial zone but only 100 kg metallic Zry in the 9^{th} zone. In both cases the melt relocation process was stopped within 100s after reflood initiation by effective cooling due to the quench front.

As mentioned in Section 2.2 the shattering model only removes all protective oxide scales in case of undamaged fuel rod segments but it does shatter neither absorber rod guide tubes (also made of Zry) nor local debris accumulations forming blockages in the coolant channel. The contribution of the absorber rods can be estimated to app. 5 % whereas the contribution of the debris (in this study only 2 axial zones) remains unclear.

5.1.2 One of each kind

For the second series of reflood cases the list of events is significantly longer (s. Table 5.2) due to the ineffective reflood process which extends the time interval in which large parts of the core remain at high temperature. Fuel rod shattering as well as absorber rod failure occurs in all three cases between 2.7m and top of the active core and extends into the fifths ring.

Core damage lasts up to 400 s where the upper third of the core remains at rather high temperatures. Therefore multi-process melt relocation occurs initiated by temperature escalation due to oxidation after shattering. App. 100 s after the first event, melt relocation continues leading to blockages at app. 2.5 m just above collapsed water level. Since S/R5 does not calculate radiative heat transfer between different axial nodes within a coolant channel, the water does not consider the presence of melt just above and, consequently no additional steam is produced.

As mentioned in Section 5.1.1 melt relocation limits code prediction in detail. The general tendency is predicted quite well, especially the risk of counterproductive measures becomes obvious. The initial benefit of reflooding the core turns to larger damage after ceasing of the LHSI pump, increasing the relocated mass to 2-3 Mg U-Zr-O. This amount seems to be small compared to masses of a molten pool of app. 80 Mg, however, it strongly influences local thermohydraulic behavior. Also decay heat, stored heat of the blockage, and the small surface to volume ration lead to worse conditions for quenching.

App. 300s after reflood initiation, PCT drops below Zry-melting point so that subsequent melting and melt relocation of U-Zr-O can be excluded. In case of a LOCA scenario with it's higher decay heat level (s. Figure 9.1) such reflood scenarios may be calculated to be not beneficial.

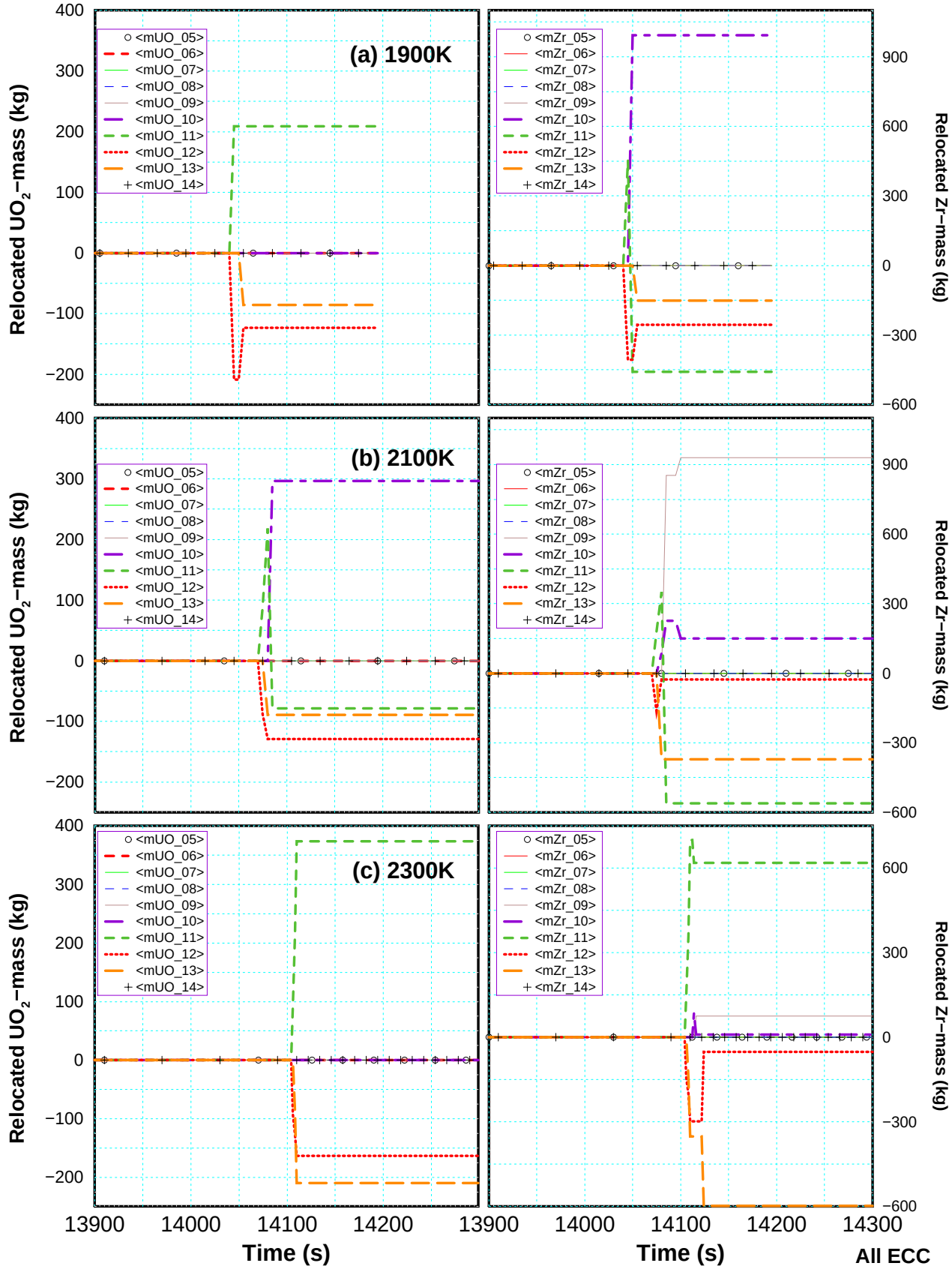

Figure 5.1 Core damage during reflood calculated for the scenario “All ECC systems” and cases: (a)1900K, (b) 2100K, and (c) 2300K, left side: UO_2 mass balance, and right side: Zircaloy mass balance.

Table 5.2 List of events for the cases: 1 MHSI + 1 LHSI with respect to: "shattering" and absorber rod failure as a function of time, axial, and radial position

Case Q1		Time sec	Fuel rod Shattering					Time sec	Absorber rod Failure and melt release				
T (K)	***t (sec)***	***Ring***	***1***	***2***	***3***	***4***	***5***	***Ring***	***1***	***2***	***3***	***4***	***5***
1700			---	---	---	---	---	13992	13/14				
			---	---	---	---	---	14005		13/14			
		Ring	***1***	***2***	***3***	***4***	***5***	***Ring***	***1***	***2***	***3***	***4***	***5***
1900		14096	12	12				14003	13/14				
Init:	14028	14060			12			14012		12			
@	14052	14066	13	11/13	11/13			14014			13/14		
.t first	14065	14155	10	10				14017		12	12		
Zone	10	14164			10			14090			10/11		
		14167	9					14091			12+14		
		14168	11	9				14098		10/11			
		14394				13		14101	10/11				
		14403			13			14222				11	
		14426					14	14344					14
		14489	14					14363					13
		14511				14							
		14524			14								
		14539	14										
		Ring	***1***	***2***	***3***	***4***	***5***	***Ring***	***1***	***2***	***3***	***4***	***5***
2100		14106			11			14003	12				
Init:	14062	14111		9				14008		13/14			
@	14088	14129	11					14011		12			
.t first	14093	14147		11				14017			13		
Zone	10	14172	10					14031			12		
		14177		10				14089	11				
		14197			10			14118				13/14	
		14212	12	12	12			14130				12	
		14224			13								
		14225		13									
		14236	13										
		14341			14								
		14376	14										
		Ring	***1***	***2***	***3***	***4***	***5***	***Ring***	***1***	***2***	***3***	***4***	***5***
2300		14155	9					14003	12				
Init:	14095	14156		9				14008		13/14			
@	14120	14176			11			14010		12			
.t first	14126	14178	11					14017			13/14		
Zone	10	14215	10					14030			12		
		14222				10							
		14227				13							
		14246		12	12								
		14253	12										
		14263		13									
		14281			13								
		14283	13										
		14402				14							
		14458		14									

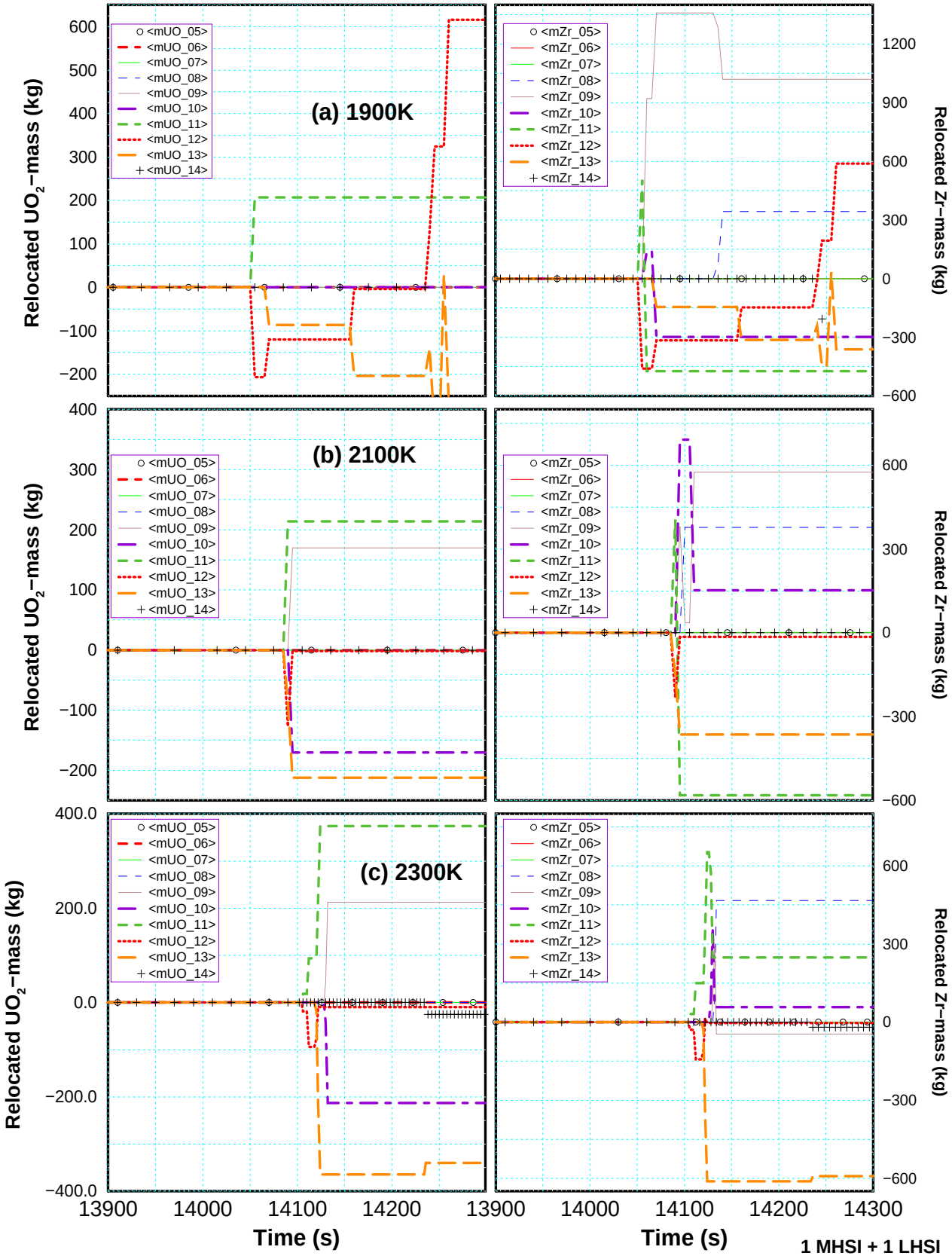

Figure 5.2 Core damage during reflood calculated for the scenario “1 MHSI + 1 LHSI” and cases: (a)1900K, (b) 2100K, and (c) 2300K, left side: UO_2 mass balance, and right side: Zircaloy mass balance.

5.2 Influence of mitigation measures

The main question is whether or not reflood is an appropriate measure to terminate or mitigate SFD accidents. From various integral experiments such as FLECHT, PKL, LOFT, etc. the capability of integral codes to simulate reflood scenarios has been demonstrated. With some code improvements, main uncertainties with respect to transition boiling heat transfer in RELAP5 has been minimized. In the following the tendency will be discussed separated for each type of injection rate ("All ECC systems" or "1 MHSI + 1 LHSI").

5.2.1 All ECC systems

In Figure 5.3 the most significant results of reflood calculations using all available ECC systems are compared to the non-mitigated accident (dotted lines). As can bee seen in the PCT (top picture), which is a measure of the superheating state, the core is cooled down rapidly. The characteristic time can be found in Table 5.1 (p. 36). The time of superheating is very short and no large damage may be triggered by additional oxidation, especially if the time scale for heat removal is considered (s. Figure 5.4). For each case the pressure built-up is shown in (Figure 5.4 a), the heat removed per second in the whole core (b), the exothermal power (c), and the total exothermal energy accumulated and released to the fluid (d).

In the 1700 K reflood case the exothermal energy released (d) is less compared to the base case (-L-) and nearly all steam is released to the PZR. In this case the heat removed reflects the stored heat in core structures (fuel rods, absorber rods, and HR).

The 2100 K reflood case shows the highest PCT and the highest hydrogen production rate of all four cases and releases most exothermal energy. This is connected with lowest steam release rate (s. Figure 5.3 and Figure 5.4) since a higher fraction of steam is consumed by oxidation (s. Figure 5.3 center), leading to 148 kg hydrogen within app. 40 s. The calculated fluid flow through safety valves is given in Figure 9.5 separately for water, steam, and hydrogen.

The exothermal energy in the 2100K case amounts to app. 20 GJ which is about twice as high as in the 1700 K case. The produced steam together with the non-condensable gas (H_2) increased the system pressure by max. 3 MPa (s. Figure 5.4 a), however, the time at high pressure is rather short.

In Figure 9.4 a summary of all hydrogen release rates from the core (top) as well as the total hydrogen mass (bottom) is shown for all scenarios in which considerable oxidation was calculated. The different water injection rates and the different initiation temperatures shift time of maximum hydrogen production between 14045s and 14130s.

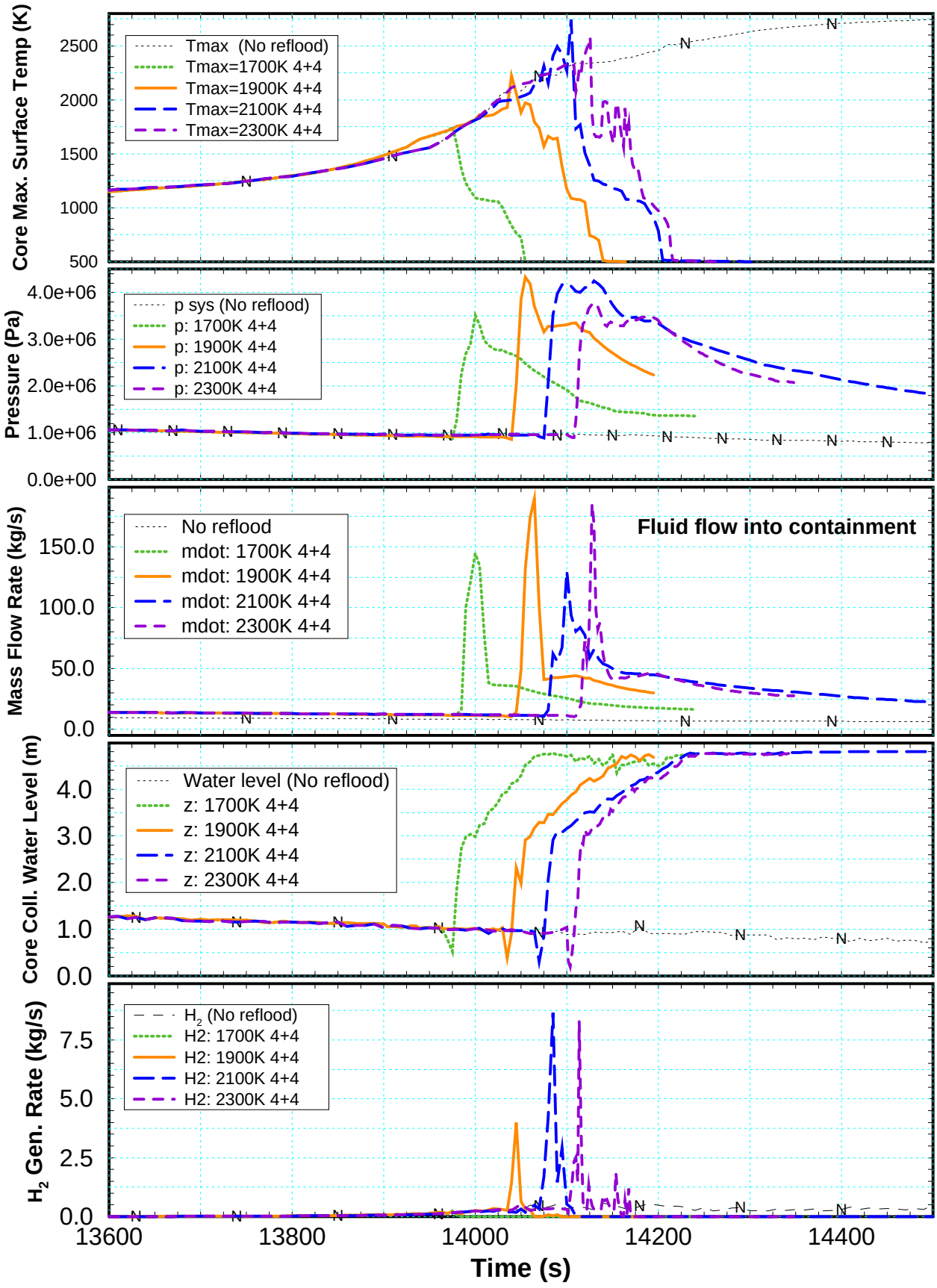

Figure 5.3 Summary of results from all calculations for the scenario “All ECC systems” activated and cases: 1700K, 1900K, 2100K, and 2300K.

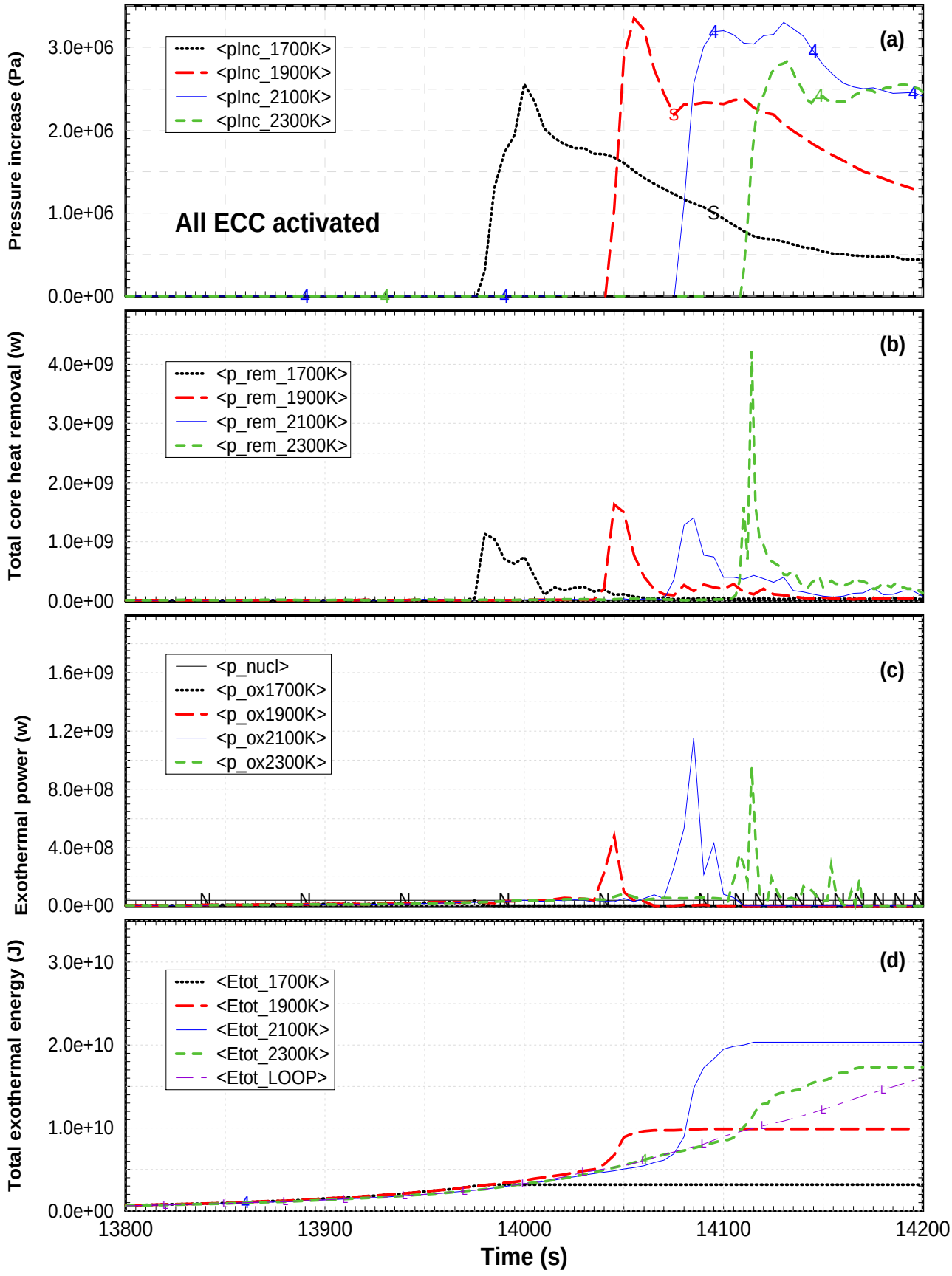

Figure 5.4 Energy balance for reflood calculations for the scenario “All ECC systems”: (a) pressure increase, (b) heat removed by fluid, (c) exothermal heat, and (d) total exothermal energy.

As already pointed out the 2300K case is already influenced by melt relocation and blockage formation so that a too detailed interpretation is not recommended.

In all cases the temperature drops steadily below 1450 K, since shattering only takes place at the phase transition of the ZrO_2 at 1473 K. After 14200s the primary system is refilled (s. Figure 5.3 bottom) in all cases and the slow pressure decrease is due to the pressure loss of water flow through surge-line and valves. As foreseen in the basic design phase vapor released from the PZR (s. Figure 5.3 center) will be condensed in the IRWST, which could not be simulated by RELAP5.

To avoid explosive H_2 concentrations the rate as well as the total mass of H_2 is important for containment safety measures. The H_2 production rate (s. Figure 5.3 bottom) shows a maximum at 2100 K and 2300 K reflood initiation temperature, prior to noticeable melt relocations in the core. At time of blockage formation interpretation of results has to stop because of model deficiencies. However, the metal available for oxidation is reduced in cases with material agglomeration and this metal is coated partially with debris. For debris situations the stored heat per hydraulic cell may be larger and the free fluid area less than for intact fuel rod regions, so that quenching is not so effective. No abnormally large releases of H_2 and thus of the exothermal energy has to be expected.

The total hydrogen mass (s. Figure 5.4 a) is higher than in the base case (LOOP) at the same time, but the unmitigated LOOP scenario continues to release H_2 leading to hydrogen mass up to 330 kg at the end of the calculation.

5.2.2 One of each kind

In this section the four reflood calculations assuming the availability of only one MHSI and one LHSI will be discussed and compared to the findings discussed in the previous section. Generally, only ¼ ECC injection rate is available, so that core cool-down can only be achieved successfully for the 1700K case (s. Figure 5.5 top). In the other cases the PCT stays for longer time periods at high temperatures, partially above temperatures calculated for the base case for the same interval.

Due to lower injection rates core cool-down to safe core state is inhibited for longer times and more steam is consumed by oxidation leading to higher H_2 production rates and masses (s. Figure 5.5). As a consequence the primary system pressure increase is less pronounced (app. 2.5 MPa, s. Figure 5.6 a) as described in the previous section (s. Figure 5.6 a). However, the system pressure remains high for cases above 1700 K. The main reason for this behavior is that the mass flow of one MHSI is too small so that practically no effective refill of the core is calculated after ceasing of the LHSI system, the reflood rates are below 1 cm/s (s. Table 5.2).

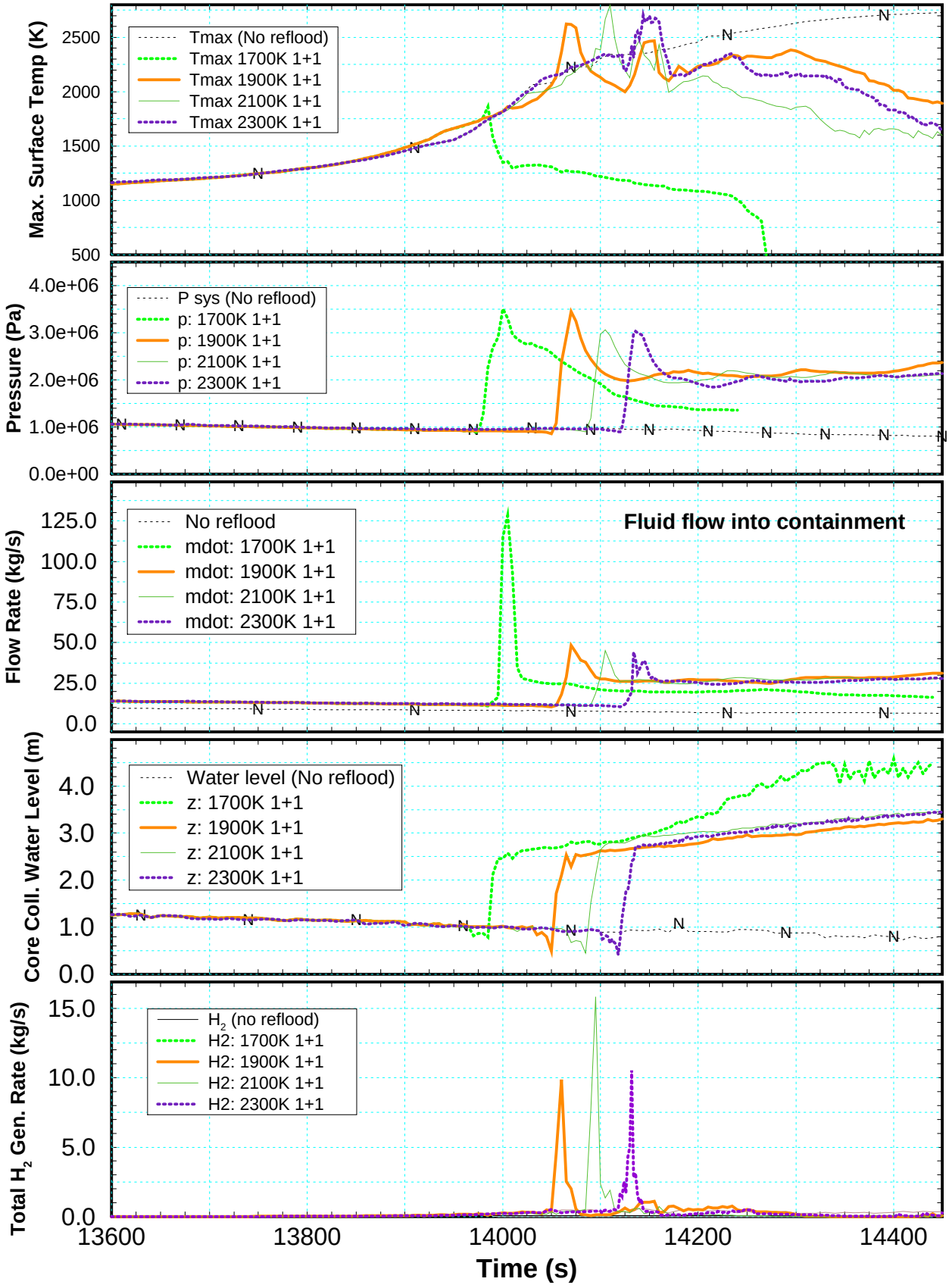

Figure 5.5 Summary of results for the scenario “1 LHSI + 1 MHSI” activated and cases: 1700K, 1900K, 2100K, and 2300K.

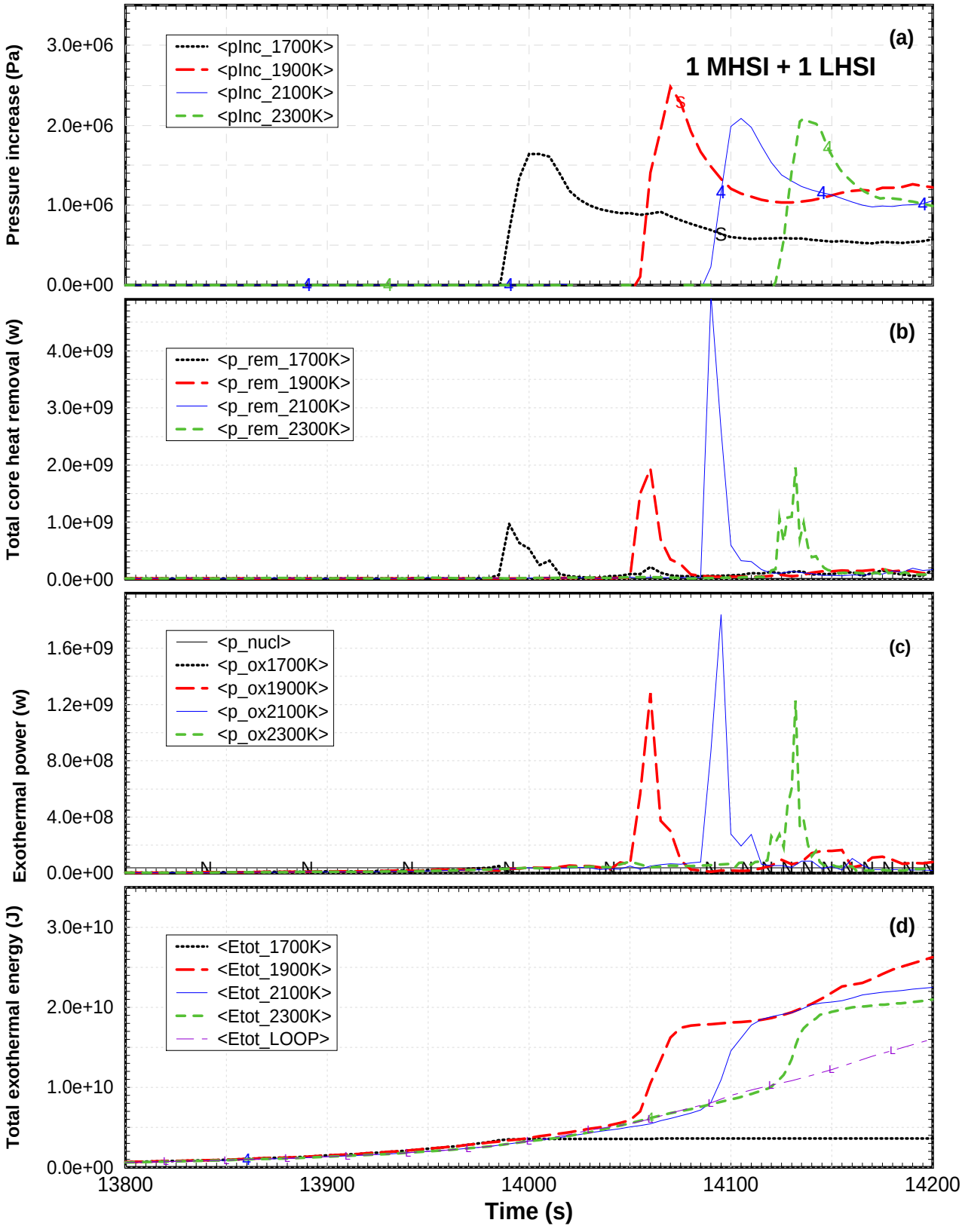

Figure 5.6 Energy balance for reflood calculations for the scenario “1 MHSI + 1 LHSI ”: (a) pressure increase, (b) heat removed by fluid, (c) exothermal heat, and (d) total exothermal energy.

The water is evaporated and consumed above by the Zircaloy oxidation. Therefore, no large steam flow rates are calculated to leave the primary system (s. Figure 5.5 center). The calculated fluid flow through the safety valves is given in Figure 9.6 separately for water, steam, and hydrogen.

For the 1700 K case no significant additional H_2 production rate is calculated (s. Figure 5.5 bottom) while the other cases show steep spikes at initial reflood (both systems injecting) and transient oxidation later-on. Flooding rates (s. Figure 5.5) are about 5-10 times smaller when compared to cases where all ECC systems feed in (s. Figure 5.3).

In Table 5.3 PCT temperatures are listed together with the steam and H_2 release rates. The tendency is that low H_2 release rates are connected to high steam rates due to low steam consumption. The system pressure build-up is then mainly affected by steam and pressure losses in the surge line. Also the core reflood velocities shown Table 5.4 represent the influence of the pressure increase, when the LHSI systems cease the velocities drop significantly. The variation in the reflood velocity in "1MHSI + 1LHSI" - 1700K case is due to fast system pressure drop so that the LHSI system continues to feed in at app. 14030s. The same was observed in 1700 K-"All ECC systems", however, the LHSI re-feed later at around 10100s when the core was nearly completely flooded. Low injection rates due to ceasing LHSI pump (only 1 MHSI pump active) lead to extreme core situations, so that for cases above 1700 K no effective core cool-down to saturation temperature was calculated.

However, the probability to activate only one of each kind is rather low, so if a common cause failure would occur either all or no ECC system will fail on request for core reflood.

Table 5.3 Summary of EPR LOOP reflood calculations focussed on hydrogen, steam production, and system pressure history.

	Initiation Temperature	Max. Temperature (K)	Max. Steam rate (kg/s)	Max. H_2 rate (kg/s)	Max. H_2 mass (kg)	Δ P sys (MPa)
All ECC	*1700K* *1900K* *2100K* *2300K*	**1850** **2250** **2700** **2550**	**150** **200** **130** **180**	**< 0.5** **4** **8.8** **8.5**	**25** **≈ 71** **≈ 148** **≈ 118**	**2.5** **3.5** **3.3** **2.8**
1 MHSI + 1 LHSI	*1700K* *1900K* *2100K* *2300K*	**1700** **2500** **2750** **2600**	**130** **50** **45** **42**	**0.5** **≈ 10** **≈ 16** **10.5**	**25** **≈ 234** **≈ 180** **≈ 192**	**2.5** **2.5** **2.0** **2.0**

The results shown here are dependent on the pressure losses in hot leg, surge line, safety valves, and piping to IRWST, as well as on the containment pressure, which have not been investigated in detail.

5.3 Parameters for QUENCH experiments

The second task of this evaluation was to derive realistic boundary conditions for the bundle QUENCH experiments performed at FZK/IMF /5/. For a simulation of a reflood process the conditions prior to reflood initiation are required, such as axial temperature profile, water level, fluid temperature, and the oxide layer thickness profile (s. Section 5.3.1). During reflood simulations two strategies can be selected: - reflood with sub-cooled water and steam production in pipes and lower zones of the test bundle, and/or – reflood with saturated water (s. Sec. 5.3.3). To perform a boil-down test in the QUENCH facility some values of the boil-down rates are given in 5.3.4.

5.3.1 Pre-quench situation

Temperatures

In Figure 5.7 (top) the axial temperature profile of the unmitigated LOOP scenario is shown for the time window of interest. At 13800s the collapsed water level is located at app. 0.9 m in the core. The temperature profile is rather flat (app. 300 K/m) below PCT of 1500 K. The heat-up rate at PCT location is app. 0.9 K/s prior to onset of temperature escalation. If oxidation starts in the upper part, average axial temperature profiles between 600 K/m and 1000 K/m can be found Then, only 200s later, two zones in the upper third exceed 2000K, so that the axial temperature profile is steepened up to 2000 K/m at 14800s. The reason for this strong temperature gradient is that the water level at 0.9 m elevation keeps the fuel rod temperatures near saturation temperature and the oxidation rises the cladding temperatures up to 2800 K above 3 m.

Furthermore, the area of beyond DBA reflood is marked in Figure 5.7 top. The lower boundary is set to 1500K the maximum PCT during DBA sequences and the upper bound is set to 2300K, above that temperature clad failure is calculated and melt relocation lead to debris formation and the available thermohydraulic models are not longer valid.

Oxidation

Strongly coupled to the axial temperature profile (s. Figure 5.7 top) is the oxide layer profile given in Figure 5.7 bottom. At 13800s the oxidation phase has just been initiated in the 12^{th} and 13^{th} axial zone and 200s later a maximum oxide layer of 50µm is calculated there. After 14000s the oxide layer thicknesses shown are influenced by material relocation transporting thermal energy to lower levels and initiating oxidation processes. Up to 14800s these local and temporal effects have leveled out and a steep increase is found, dividing the core into two zones, a lower one with temperature, below 1200 K, and a higher one (above 3 m) with high temperatures and oxide scales up to 350 µm. The value at 3.2m (11^{th} axial zone) is affected by earlier melt relocation stopping clad oxidation at app. 70µm, however debris oxidation is still going on. After 14800s debris formation and transition to molten pool follows.

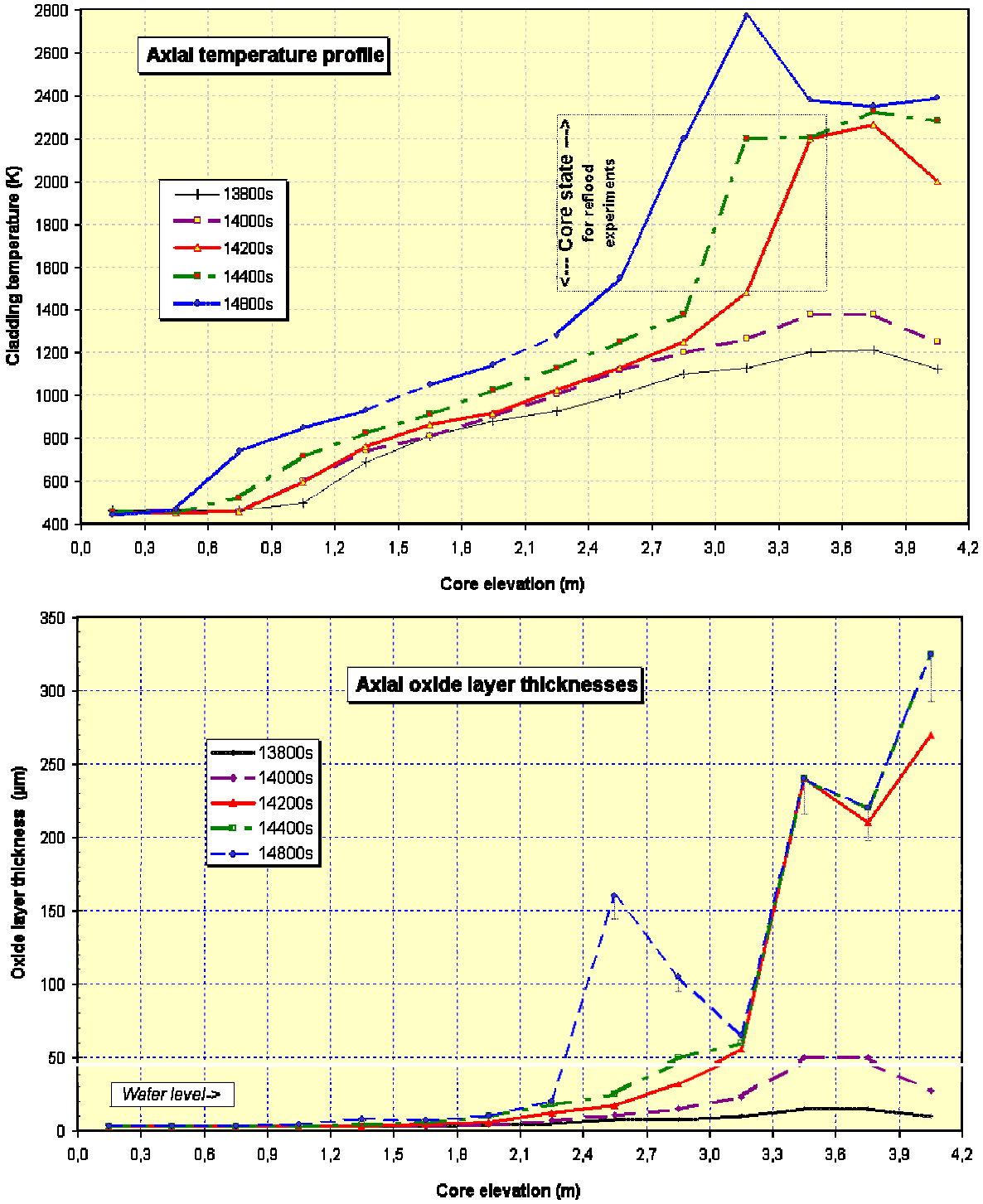

Figure 5.7 Temperature (top) and oxide layer thickness (bottom) development for the base case (unmitigated LOOP) scenario at times when reflood was calculated for the different cases of this study.

5.3.2 Conditions for water reflood

Taking into account the coarse prediction of the shattering model, it can be stated that in scenarios where “All ECC systems available” the reflood is finished within less than 130s (s. Table 5.4). Hydrogen and steam is produced but significantly less than in the “1 MHSI + 1 LHSI” cases. Reflood rates are rather high also in the upper half of the core where only the MHSI sys-

tems contribute to the effective reflood rate. In case of melt relocation the prediction of the calculation has to be interpreted more carefully, but cool-down to a safe core state has been calculated in all cases.

In the cases "1 MHSI + 1 LHSI" this can only be stated for reflood initiation temperatures at 1700 K and below. At 1900K and beyond, oxidation, melt relocation, and debris formation lead to a core state which cannot be handled by the actual code generation. On the other hand codes dedicated for debris reflood calculations are not applicable to such a scenario since in the core all states from intact fuel rods to cohesive debris vary.

Table 5.4 Summary of EPR LOOP reflood calculations showing flooding velocities in different parts of the core

	Initiation Temperature (K)	**Reflood initiation time (m s)**	**Flooding velocities in the core (cm/s) Lower half - Upper half**		**Time to safe core state (s),**
T_{max} ROD			**< 1200 K**	**1400-2400K**	**($T=T_{sat}$)**
All ECC	*1700K* *1900K* *2100K* *2300K*	*232m 45s* *233m 48s* *234m 22s* *234m 55s*	**15** **12** **15** **20**	**2.5** **1.8** **1.3** **1.5**	90s 120 s 140 s 130 s
1 MHSI + 1 LHSI	*1700K* *1900K* *2100K* *2300K*	*232m 45s* *233m 48s* *234m 22s* *234m 55s*	**17** **12** **15** **11**	**0.3- 1.04** **≈ 0.2** **≈ 0.13** **≈ 0.21**	300 s > 500 s > 600 s > 600 s

Due to the low ECC injection rates, the effective reflood rate is reduced by evaporation and the amount of steam again by oxidation, so that a hot steam / hydrogen mixture was calculated to leave the core. With respect to containment hydrogen mitigation measures, such a mixture is critical due to the high hydrogen and low steam concentration.

5.3.3 Conditions for steam reflood

One possibility to separate effects is to simplify the conditions in the fluid channel. In single effect quench tests with steam cooling it was found that similar phenomena occur leading to hydrogen production during cool-down.

For steam quenching experiments in the QUENCH facility typical steam flow rates at or just above saturation temperatures have to be derived from the calculations. Steam flow rates vary from one case to another due to evaporation rate and steam consumption due to oxidation.

In Figure 5.8 steam mass flow rates are given for all four cases of "All ECC systems" for one representative fuel rod in the 3rd ring of the core at core height of 3.6m and 4.0m where the highest temperatures are reached prior to reflood. To get rid of numerical oscillations the results are filtered by gliding averaging.

The general tendency is that after the first spike, caused by injection of both systems, the steam mass flow levels out to values oscillating at 2-5g/(s.rod) until the core becomes flooded. Negative values indicate local pressure differences mainly affected by strong hydrogen production in the vicinity. The void profiles in this core channel are shown in the appendix (s. Figure 9.7). Here it becomes clear that even at 3.5 m (void_3m5) droplets exist app. 50 s after first rise of water level in the core. So the time period for pure steam cooling is rather short and no significant cool down is calculated for the upper third of the core (s. Figure 4.7 and Figure 4.8).

For the other scenario "1 MHSI + 1 LHSI" the same shape of the curves can be found in Figure 5.9, only the maximum values are scaled down as expected. Comparing both figures the influence of the thermohydraulics onto the steam mass flow rate becomes evident. In cases of "1 MHSI + 1 LHSI" no strong oscillations are present app. 300 sec after the initial steam peak. Later on, especially in the 2300K case, oscillations grow mainly due to the formation of local debris which strongly influences evaporation due to different masses and fuel-wall interface areas in each zone. In this case predictions of the code are questionable.

Void profiles in this core channel are shown in the appendix (s. Figure 9.8). In the four cases steam cooling above 3.5 m extends between 240s (1700K case) and more than 400 s (2300K case) leading to high cladding temperatures as can be seen in Figure 4.10 and Figure 4.11. Two reasons are responsible for that calculated behavior.

- Low water injection rate (G < 1g/(s.rod)) leads to low evaporation rate,
- High surface temperatures enhance steam consumption by oxidation

Based on these findings and the properties of the QUENCH facility, a steam quenching experiment should simulate two phases: initial steam spike with > 5 g/(s.rod) steam flow rate and the cool-down phase with 2-3 g/(s.rod) steam flow rate of saturated steam up to the end of the experiment, global cool-down to saturation temperature.

Taking into account shroud and instrumentation tubes the fuel rod bundle consisting of 21 fuel rods has to be extended by 2 for the instrumentation plus app. 5 for the shroud. So the total flow rate should be in the range of : initial spike 150 g/s for 30s and 56 g/s steam flow rate of saturated steam up to global cool-down to saturation temperature.

5.3.4 Conditions for boil-down

For the preparation of boil-down tests, the velocity range calculated for the core is required. In the appendix in Figure 9.3 steam mass flow rate at core exit, collapsed water level, as well as the averaged boil-down or evaporation rate are given. A maximum boil-down rate of –0.21 cm/s is calculated between 3.5 m and 4.0 m. Together with a minimum value of –0.03 cm/s in the lower half of the core, a mean value of -0.088 cm/s (app. 5 cm/min) is computed in the time interval between 3.2 and 4.4 h after scram.

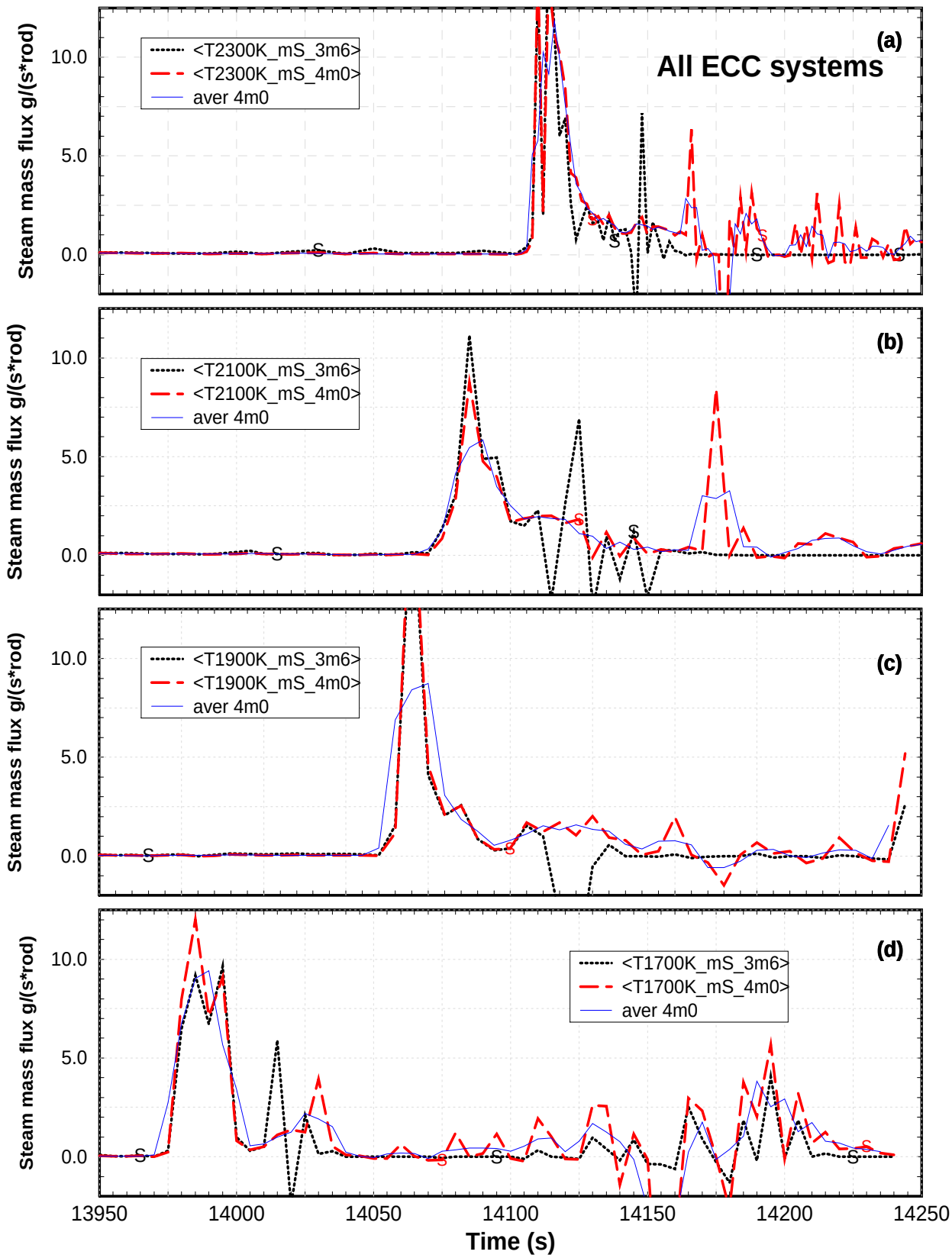

Figure 5.8 Steam mass flow rates in the core 3rd channel for scenario “All ECC systems” for reflood cases: (a) 2300K, (b) 2100K, (c) 1900K, and (d) 1700K.

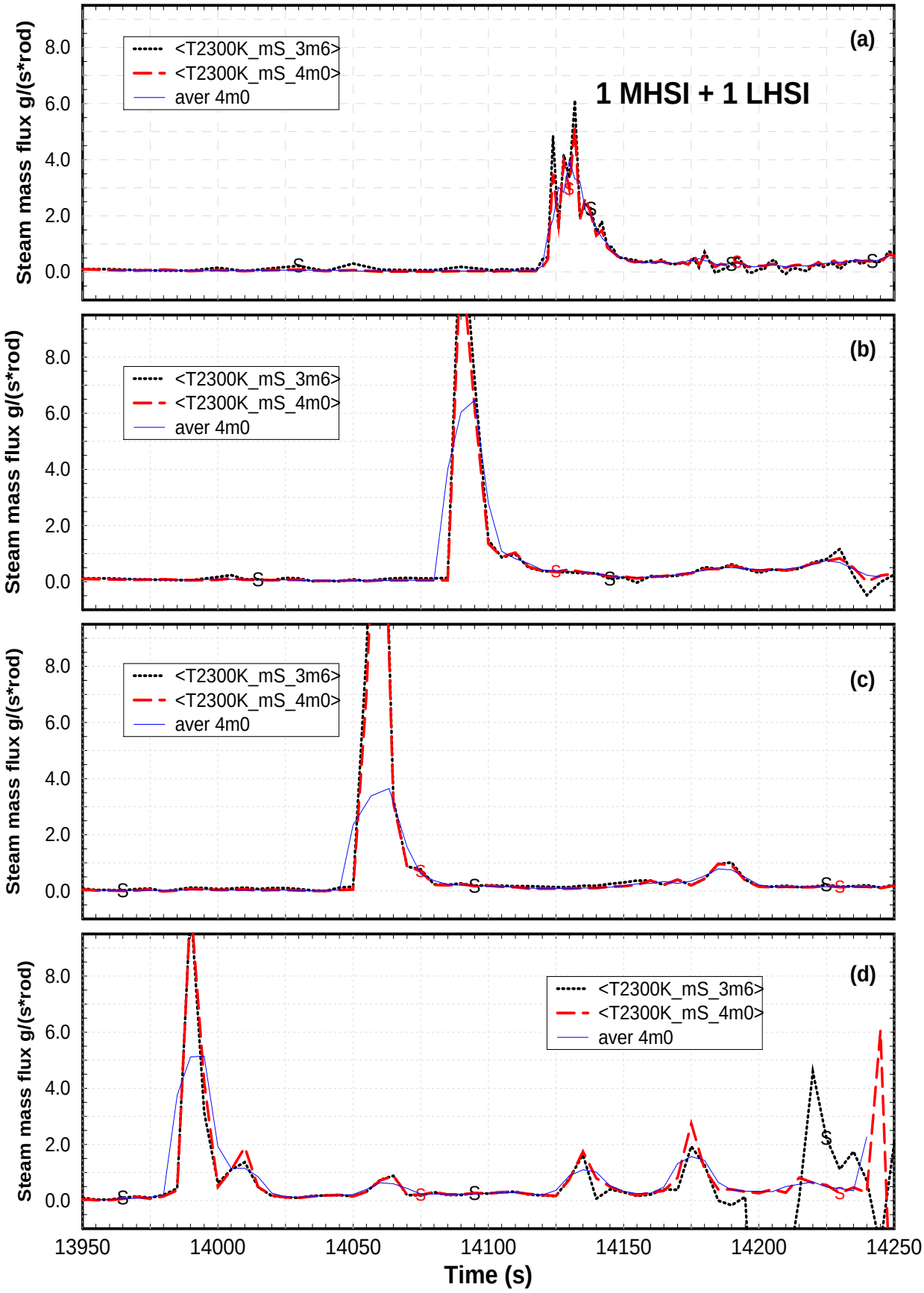

Figure 5.9 Steam mass flow rates in the core 3rd channel for scenario 1 MHSI + 1 LHSI for reflood cases: (a) 2300K, (b) 2100K, (c) 1900K, and (d) 1700K.

6 SUMMARY AND CONCLUSIONS

The influence of reflood initiation times prior to melt relocation and availability reflood capabilities on the cool-down process has been investigated using SCDAP/RELAP5 mod 3.1.F, an improved version of the USNRC code system. As base case scenario the loss-of-off-site power has been selected. Time of first reflood initiation was set to 3.8 h after scram. The calculations start with DBA conditions and end with reflood initiation at a PCT of 2300K. At those temperatures melt relocation has not yet been initiated, however, during reflood massive oxidation and melt relocations were calculated to occur.

Below 1700 K PCT the conditions can be handled by DBA code systems reliably, since no noticeable oxidation and melt relocation is calculated to take place. Above those PCTs oxidation strongly influences the reflood process and beyond 1900 K melt relocation complicates conditions in the fluid channel.

The main question has been answered based on state of the art modeling in severe fuel damage. Reflood calculations show that if a reflood is initiated in the early core melt phase the reflood capability of the systems should be high enough to cool-down the core in a short period of time. If this cannot be achieved, severe core damage may be ongoing partially enhanced by fragmentation processes due to thermal shock of the oxidized claddings. This may be important to establish additional on-site reflood capabilities.

Values for hydrogen production are based on the coarse fragmentation model (shattering) and reflect an upper bound due to the chosen conservative assumptions. Hydrogen production rates rank between 3 kg/s and 16 kg/s depending on scenario and reflood initiation temperature. The total amount of hydrogen, however, is less that the unmitigated accident would release. Presently results of the QUENCH programme are not incorporated in fragmentation modeling since the basic processes have not been identified clearly.

With respect to conditions for experiments in the integral QUENCH facility, a set of parameters can be depicted from this study. A typical value for the axial temperature profile in the core prior to reflood is 500 –700 K/m. Heat-up rates necessary to achieve typical oxidation profiles should be less than 1 K/s (at 1500 K) at the hottest zone of the core. Reflood velocities in the core for worse case simulations should be 0.5 – 1.0 cm/s, the reflood water temperature is slightly below saturation due to mixing with the remnant water in the lower plenum and the core. For steam quenching an initial spike with $G > 5$ g/(s.rod) steam flow rate and in the cool-down phase with G app. 2-3 g/(s.rod) steam flow rate of saturated steam up to global cool-down to saturation temperature should be chosen.

Another important finding is, that the fragmentation model should be improved based on the experimental findings from the QUENCH programme and implemented into SCDAP/RELAP5 mod3.2 to take credit from the RELAP5 reflood capabilities developed at PSI.

7 ACKNOWLEDGEMENT

I would like to thank Dr. Christoph Homann (FZKA/IRS), Dr. Dankward Struwe, and Herrmann Plank (Siemens/KWU) for their thorough review of the paper and valuable remarks.

8 LITERATURE

/1/ Golden, D. W., TMI-2 Analysis Exercise Final Report, ref. DWG-07-90, published by EG&G, 1990.

/2/ Coryell, E. W., Summary of Results and SCDAP/RELAP5 Analysis for LP-FP2, NUREG/CR-6160, April 1994.

/3/ Comparison of the Quench Experiments CORA-12, CORA-13, CORA-17, S. Hagen et. al. FZKA-5679, August 1996.

/4/ P. Hofmann et. al., Physico-Chemical behavior of Zircaloy Fuel Rod Cladding Tubes During LWR Severe Accident Reflood, FZK-5846, 1997.

/5/ P. Hofmann, C. Homann, W. Leiling, A. Miassoedov, D. Piel, L. Schmidt, L. Sepold, M. Steinbrück, Results of the QUENCH Commissioning Tests, FZKA 6099, August 1998.

/6/ C. M. Allison et al.: SCDAP/RELAP5 mod3.1 Code Manual, Vol. I-IV. NUREG/CR-6150, EGG-2720, Oct. 1993.

/7/ W. Hering, EPR-Kernschmelzanalysen mit SCDAP/RELAP mod 3.1, PSF-Bericht 1999.

/8/ W.Hering, C. Messainguiral, Improvement of the SCDAP/RELAP5 Code with respect to the FZK QUENCH Facility, FZKA, 1999.

/9/ H. Plank, private communication 1997.

/10/ W. Hering, W. Sengpiel, D. Struwe: Calculation of Bundle Degradation in the Phebus FPT0 In-pile Experiment with SCDAP/RELAP5, Annular Meeting on Nuclear Technology ‘96, Mannheim, Germany, March, 21-23 1996.

/11/ E. Elias, V. Sanchez, W. Hering; Development and validation of a transition boiling model for RELAP5/MOD3 reflood simulations, NEDEA 183 177-332 (1998).

/12/ J.C. Chen, R.K. Sundaram, F.T. Ozkaynak, A phenomenological correlation for post-CHF heat transfer, Lehigh University, NUREG-0237, June 1977.

/13/ S.-O. Smit, W. Sengpiel, W. Hering, Investigation of the Phebus FPT0 bundle degradation with SCAP/RELAP5, FZKA 6083, April 1998.

/14/ Ch. Homann, W. Hering, W. Sengpiel, D. Struwe, C. Messainguiral: Analysis of LWR Fuel Rod Bundle Experiments with SCDAP/RELAP5, 1996 RELAP5 International Users Seminar Dallas, TX, USA, March, 17-21 1996

/15/ Ch. Homann, W. Hering, V.H. Sanchez: State of FZK/IRS calculations for the projected QUENCH facility, 2. International QUENCH workshop, Karlsruhe, September 16-19 1996.

/16/ Hering, W.; Homann, Ch.; Sanchez, V.H.; Sengpiel, W.; Smit, S.O.; Hofmann, P.; Steinbrück, M.; Piel, D.; Schmidt, L.; Messainguiral, Ch. Untersuchungen Zur Kernzerstörung. Nachrichten - Forschungszentrum Karlsruhe, 29(1997) S.309-326

9 APPENDIX

9.1 Options of reactor safety system

Table 9.1 Trips to simulate the reactor safety system necessary for EPR calculations

Trip setpoints					
10				Primary system pressure	p prim < 13.25 MPa
11				Delay signal 10 for 0.8 sec	
12				Pump velocity too low	Pump velocity < 101.1
13				Delay signal 12 for 0.6 sec	
22				2nd side pressure in SG to high	p sec > 9.15 MPa
31	32			SG water level too low	< 13m
35	1030			Delay signal 1033 for 0.6 sec	
1099	1011	1012		Reactor scram setpoint summary	11 - 13 - 22 - 25
Initiation					
100			1100	Time for break initiation	USER value
101			1101	Time for surge line valve closure	USER value
102			1102	Time for loss of off-site power	USER value
103			1103	Max core temperature exceeded	T core > 4444
104	105		1104	SIS actuation	PCT > $T_{(USER)}$
Accumulator					
111	112			Accu initiation	p prim < 0.45 Mpa
1111	1112			Accu surge line valve open	p prim < 0.45 Mpa
Decay heat					
199				Start decay heat calculation	Delay signal 1099 for 0.5s
Secondary side insulation					
302	303			Delay signal 1099 for 2.0 and 2.5s	
1301	1302	1303		Scram and turbine insulation	
1401				MFWS trip from 1099	
Primary side pressure control					
601			1601	Close PZR surge line if water volume < 0.5 m³ (for SL-rupture)	
620	621			Overpressure control valve 824	17,6 MPa > P > 16.6 MPa
630	631			Overpressure control valve 834	18,0 MPa > P > 17.0 MPa
Primary side depressurization control					
622	623			Vapor Temperature	T_F (202, 203) > 923 K
1625	1626			Valve actuation 824	
1635	1636			Valve actuation 834	
304	305			2nd side pressure in SG too high	p_{sec} > 9.15 Mpa
1304	1305			or SIS actuation from signal 1104	

9.2 Decay heat

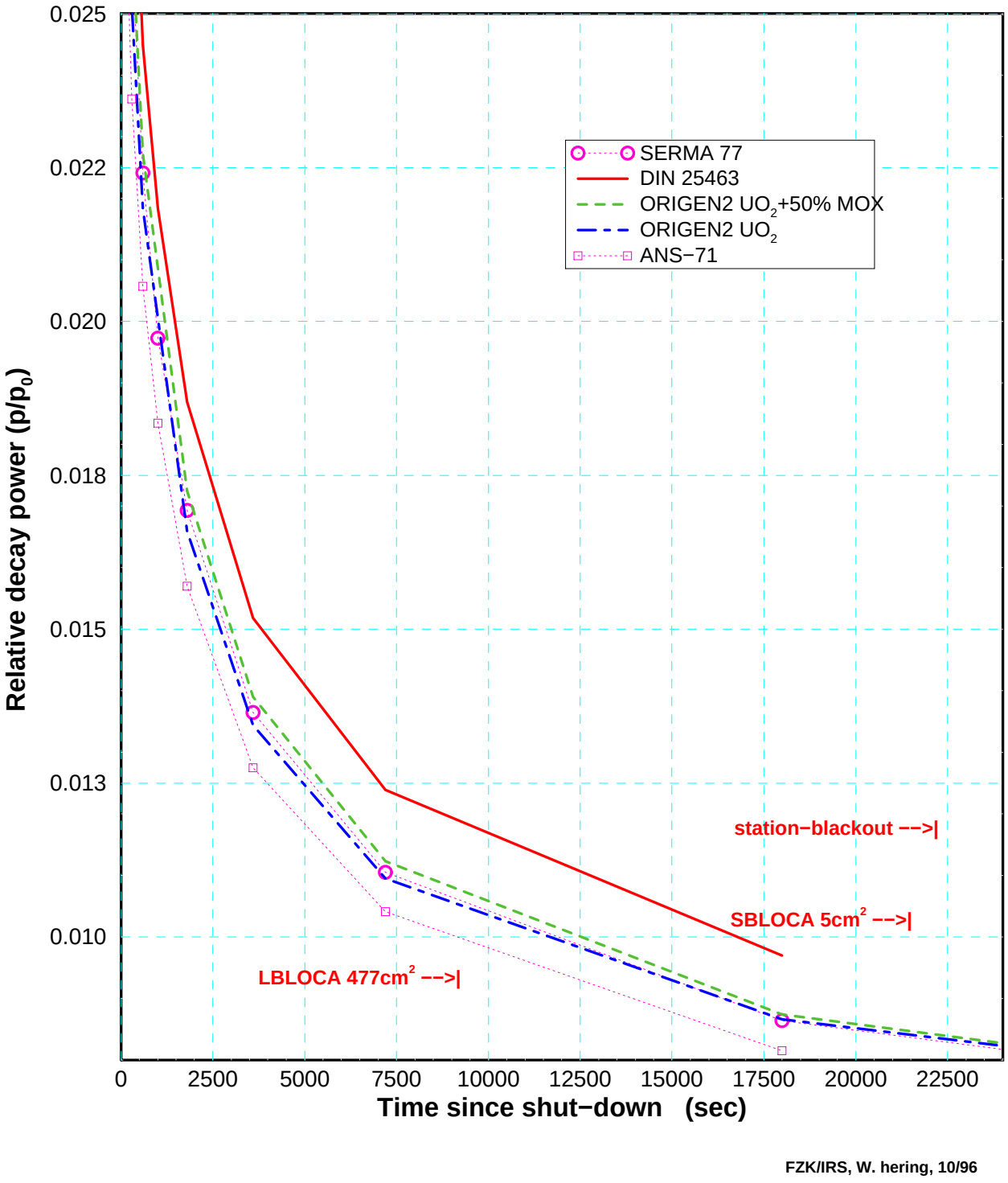

Figure 9.1 Decay heat curves for simulation. The SERMA 77 was used for the calculations performed for this study.

9.3 Core temperatures of LOOP base case

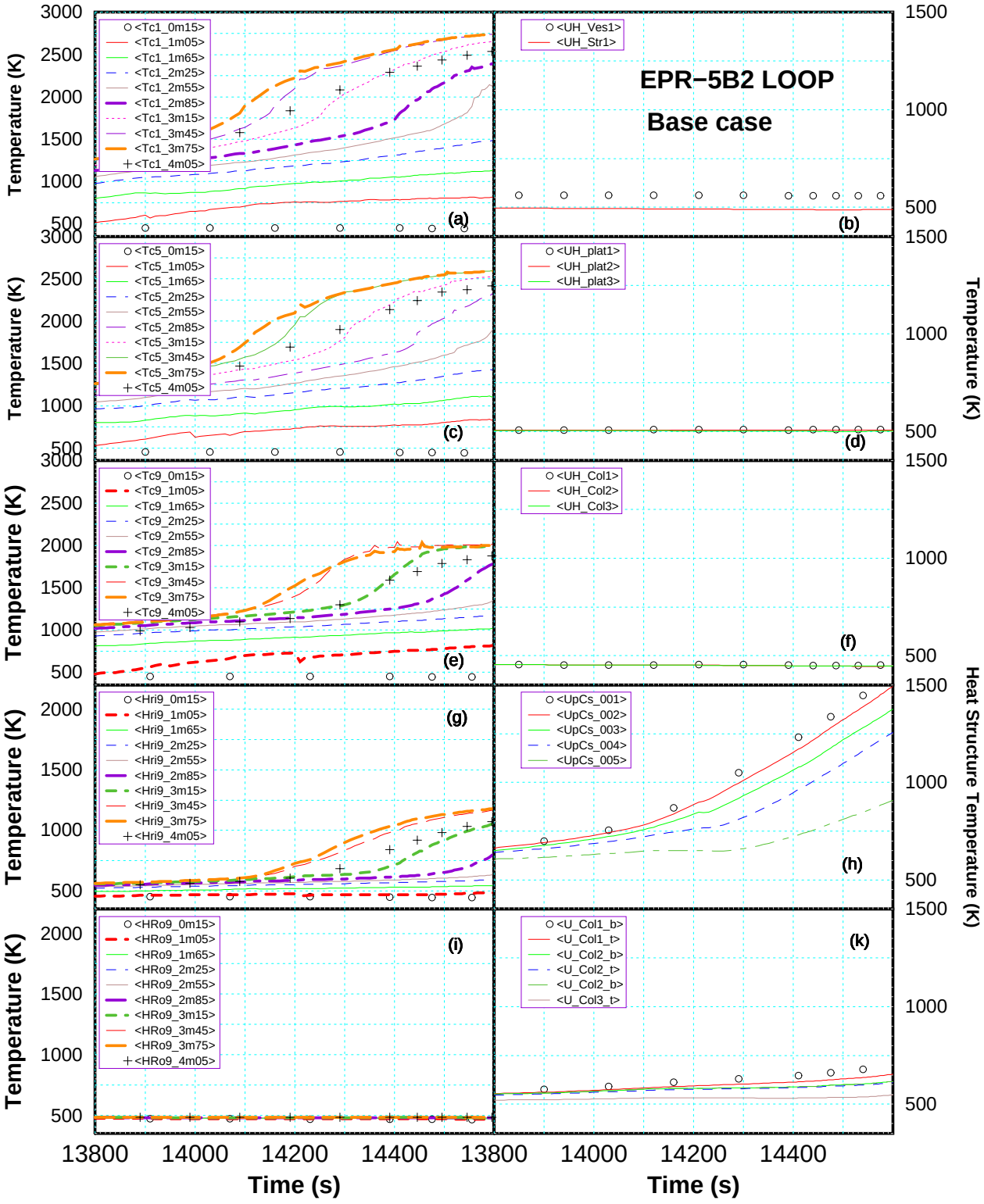

Figure 9.2 Temperature history of the unmitigated LOOP scenario: core temperatures (left) and upper plenum internals (right)

In Figure 9.2 the cladding temperatures of the first ring (a), of the 3rd (c), the 5th ring(e), the heavy reflector inner (g) and outer surface (i) temperatures are given for the time window of re-

flood calculations. For indicated elevations (4m05 = 4.05 m). On the right side temperatures of vessel structures are given: upper head (b), the upper support plate (d), the absorber rod guide tube in the upper plenum (f), the upper core plate (h), and the lower core plate (k).

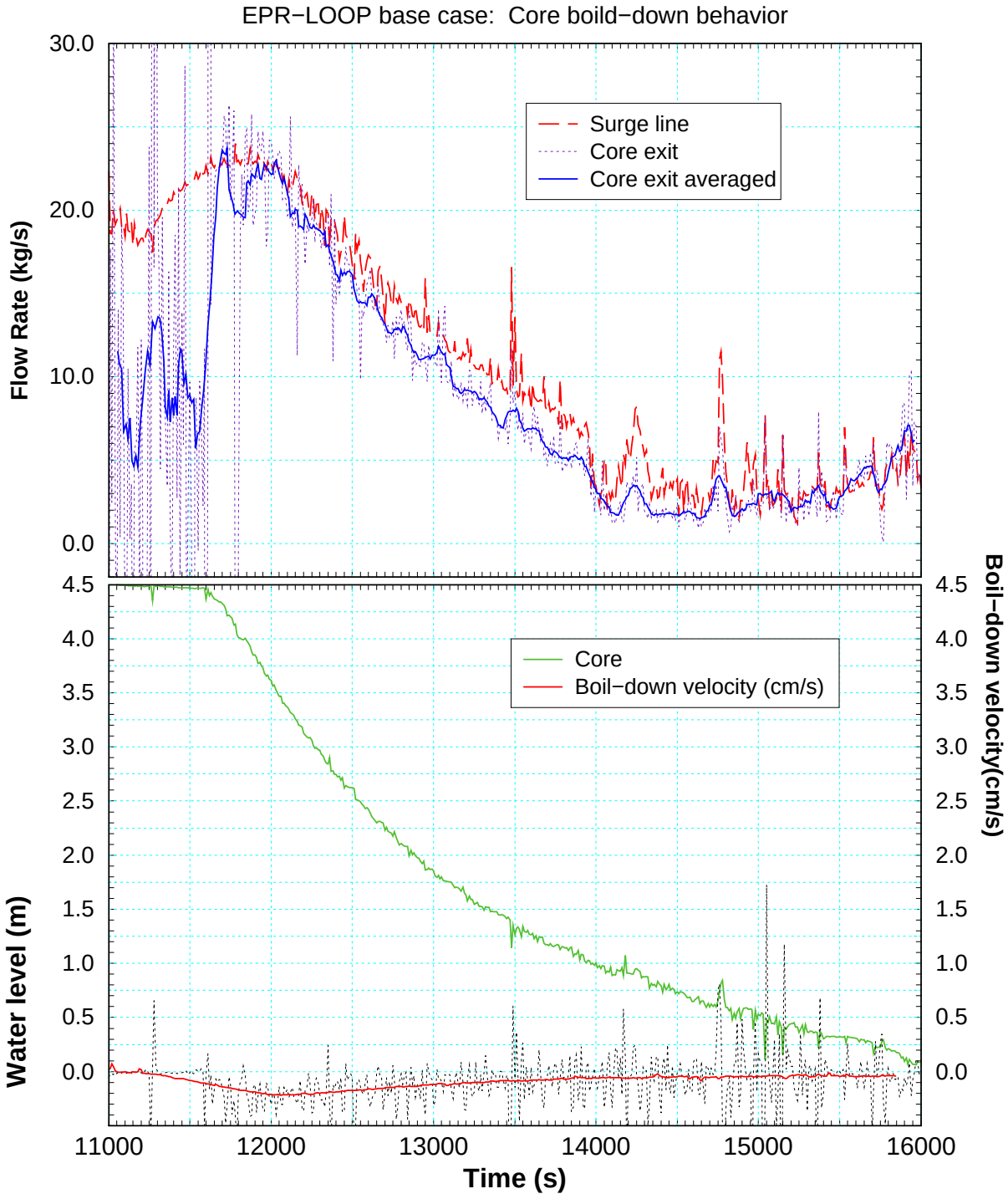

Figure 9.3 LOOP base case mass flow rates at core exit and in surge line (top) and water level and boil-down rate in the core (bottom).

9.4 Additional reflood results

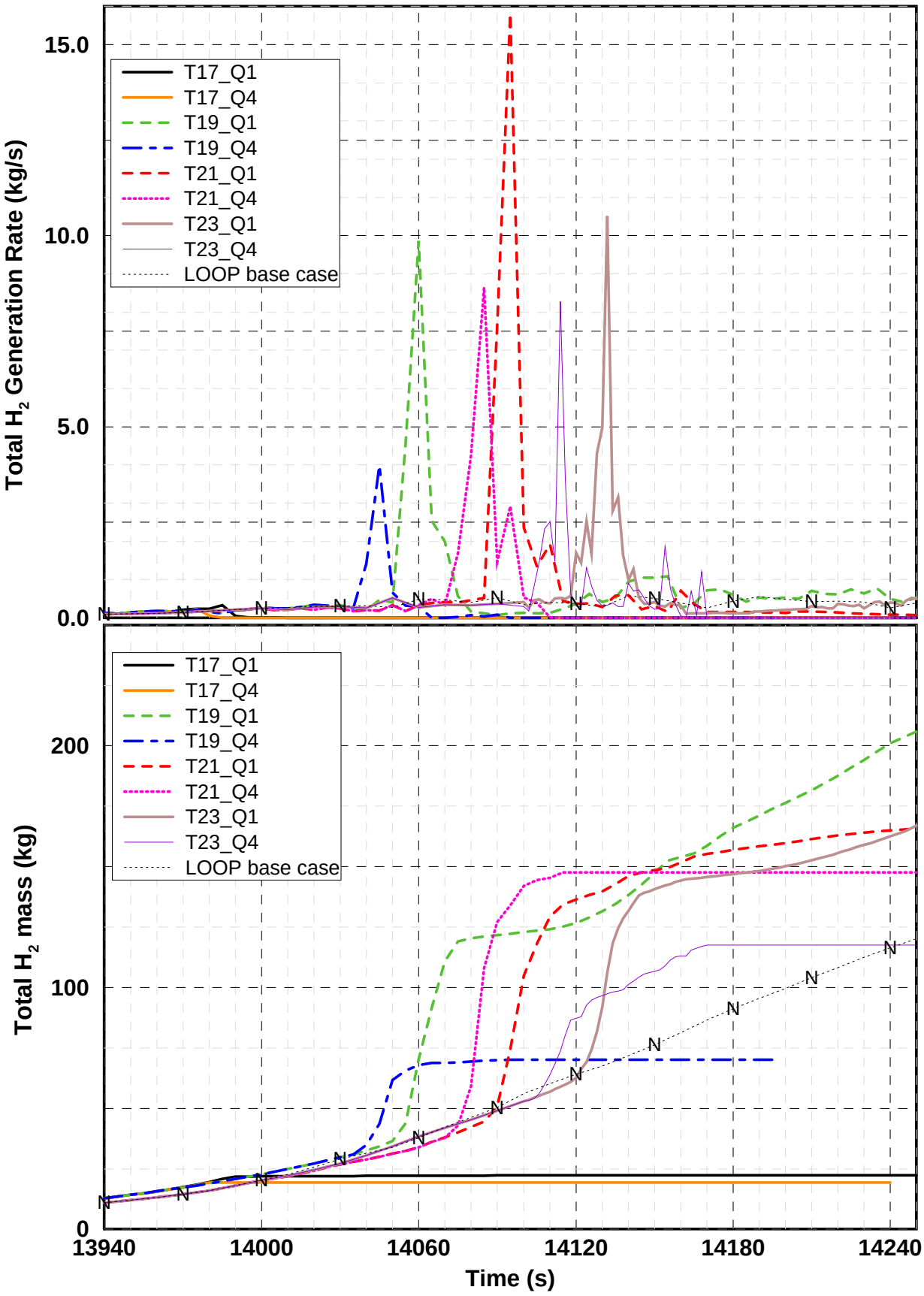

Figure 9.4 Summary of all hydrogen data, top: production rates in the core, and bottom: total hydrogen mass.

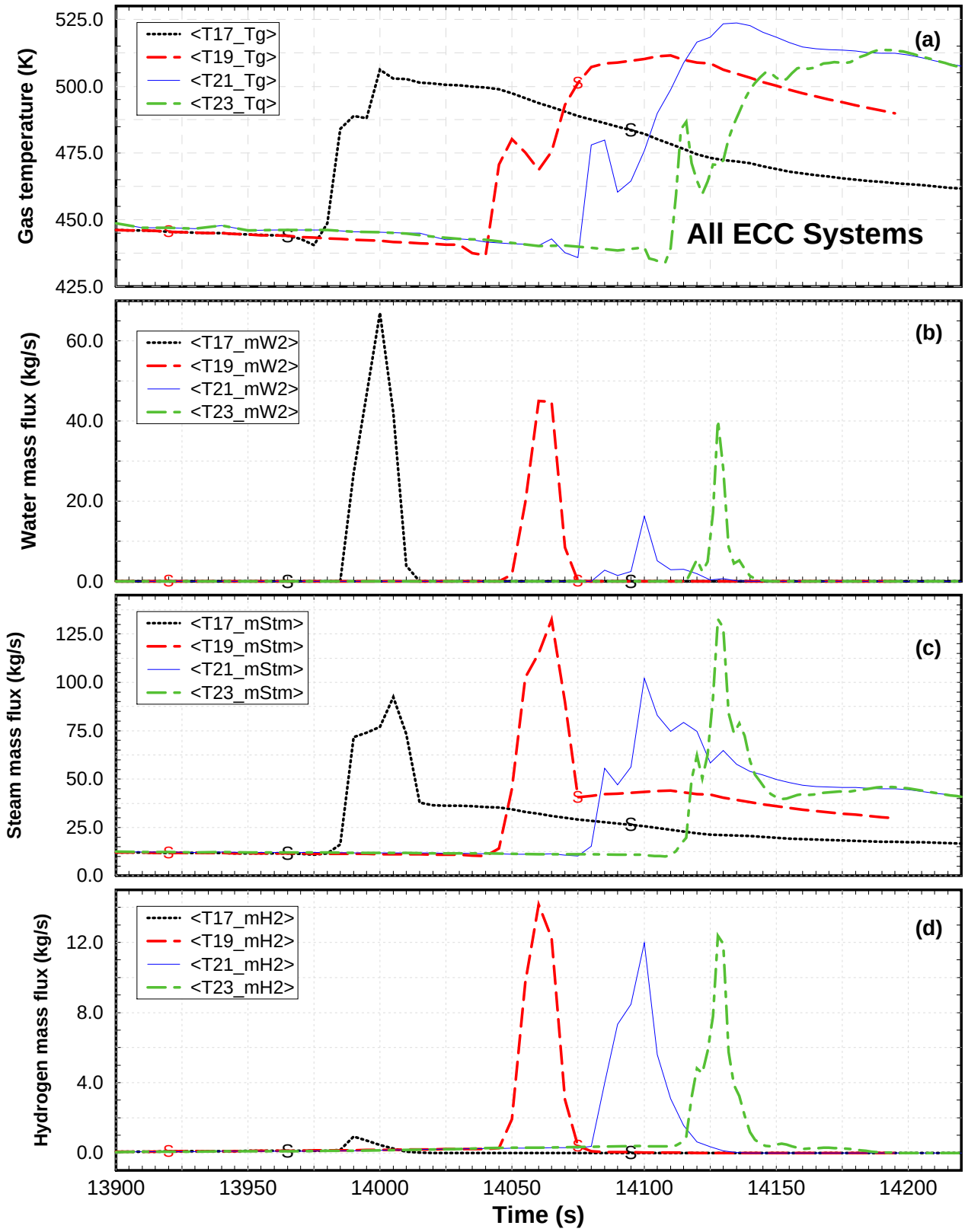

Figure 9.5 Fluid state at pressurize safety valve for the scenario All ECC Systems: (a) gas temperature, (b) water mass flow, (c) steam mass flow, and (d) hydrogen mass flow out of primary circuit.

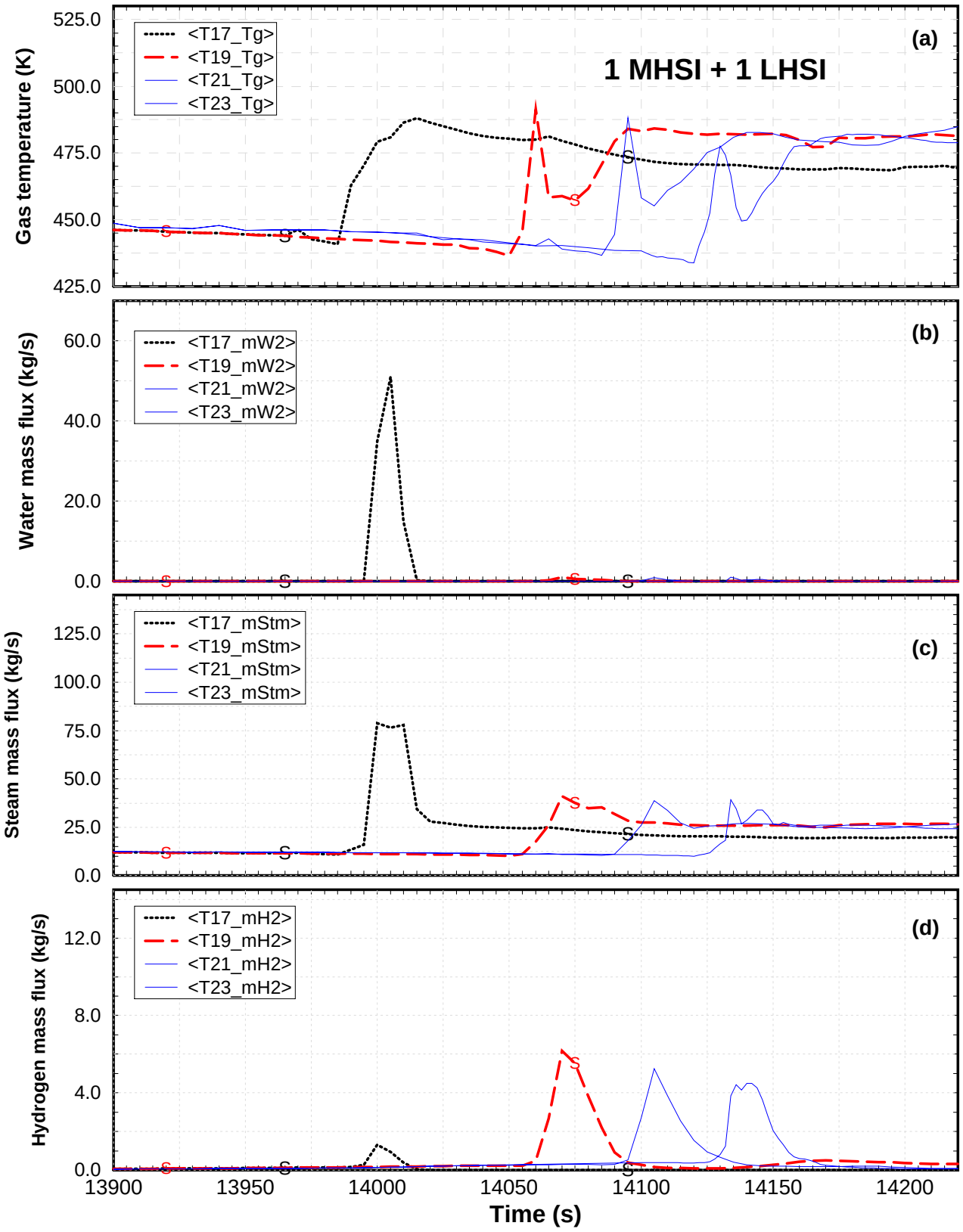

Figure 9.6 Fluid state at pressurize safety valve for the scenario 1 MHSI+ 1 LHSI : (a) gas temperature, (b) water mass flow, (c) steam mass flow, and (d) hydrogen mass flow out of primary circuit.

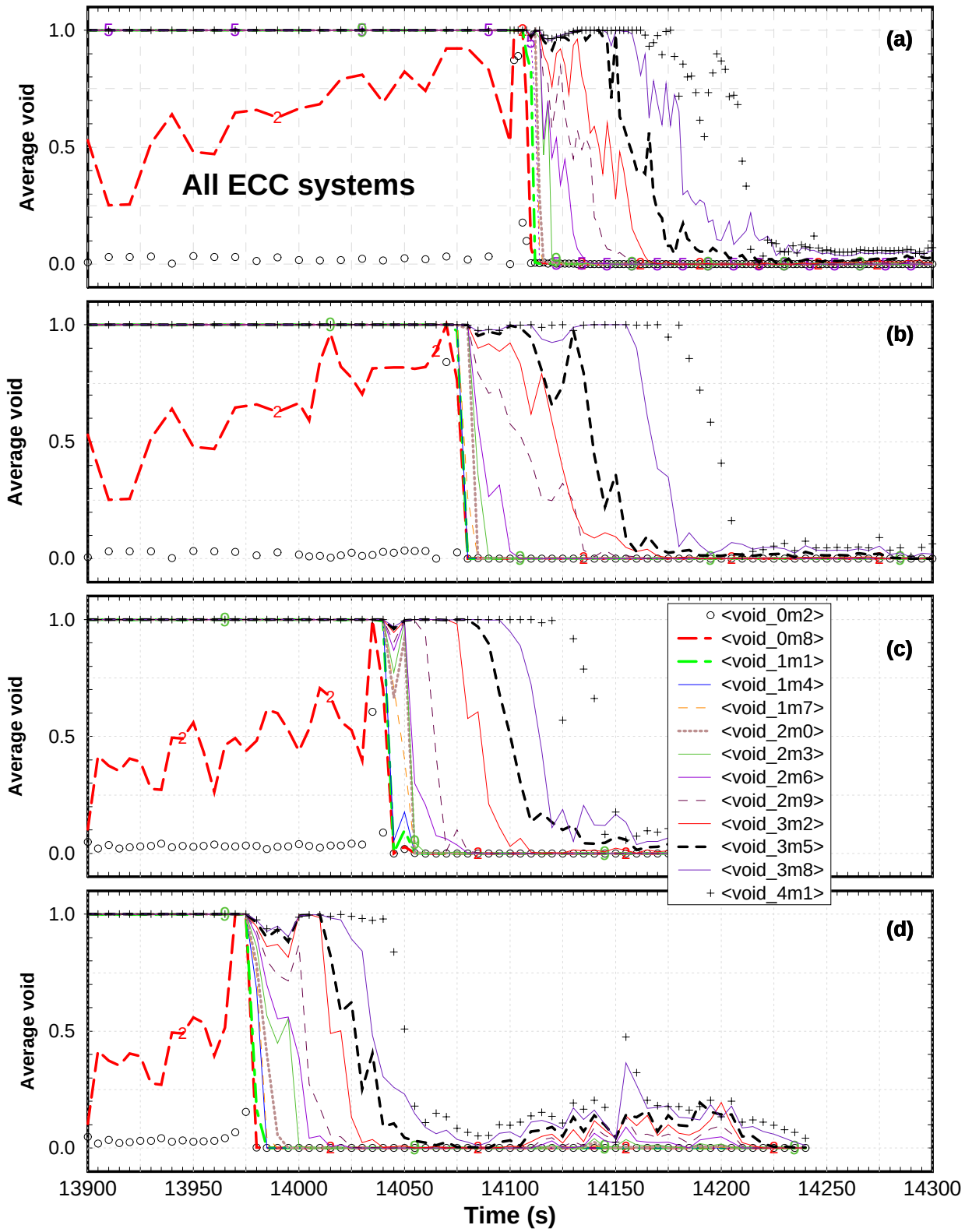

Figure 9.7 Average core void for cases “All ECC activated”,
for reflood cases: (a) 2300K, (b) 2100K, (c) 1900K, and (d) 1700K

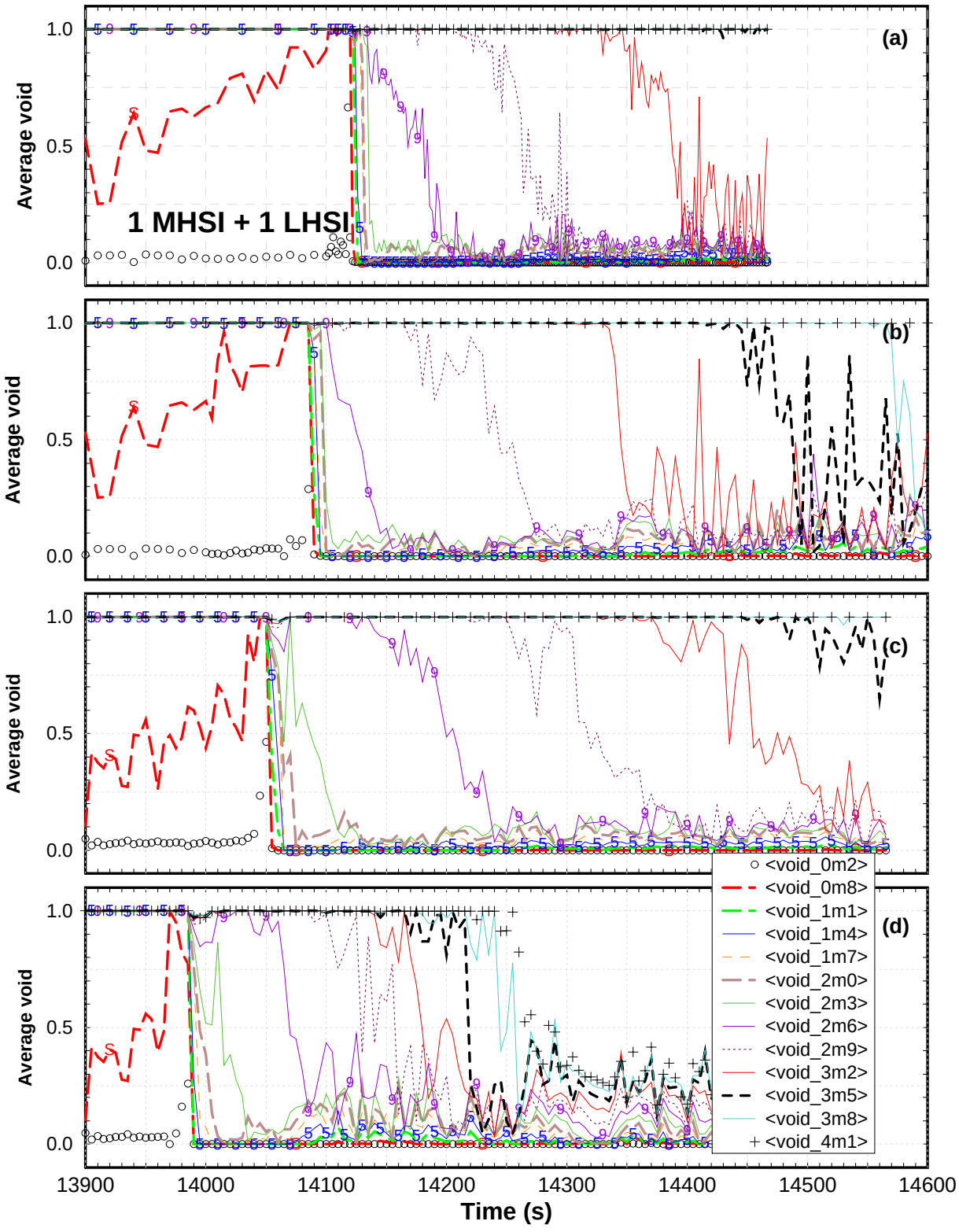

Figure 9.8 Average core void for cases "1 MHSI + 1 LHSI"
for reflood cases: (a) 2300K, (b) 2100K, (c) 1900K, and (d) 1700K